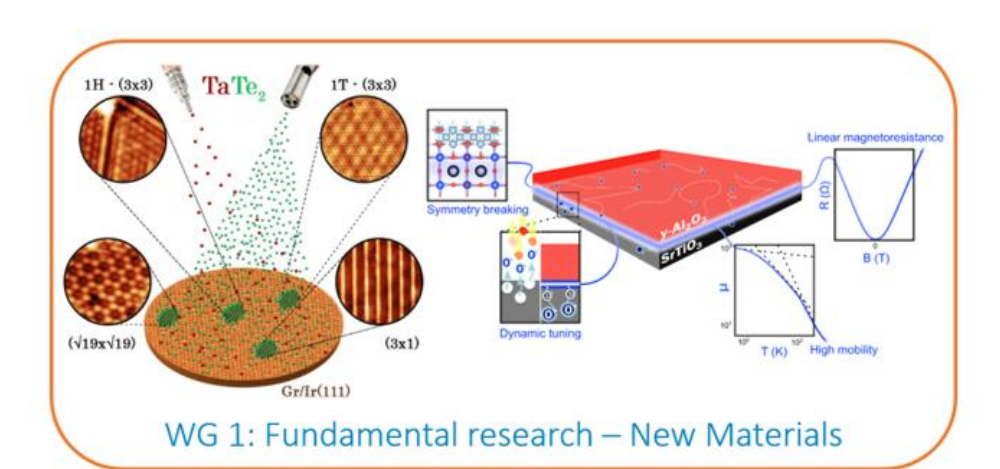


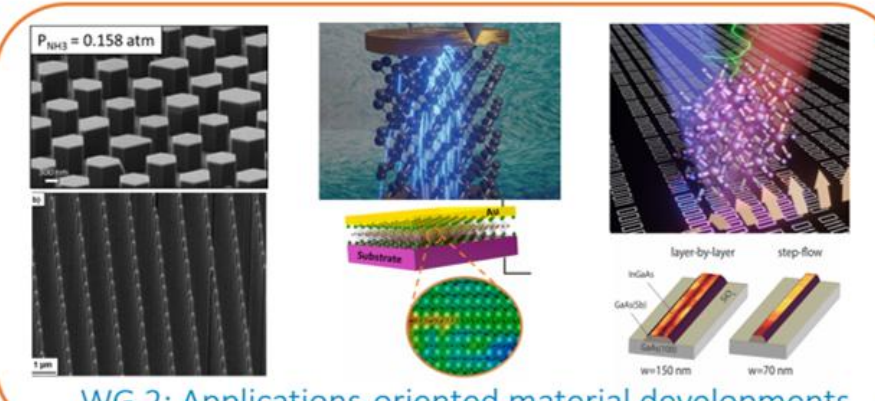
European Network for Innovative and Advanced Epitaxy "OPERA" COST Action

https://cost-opera.eu

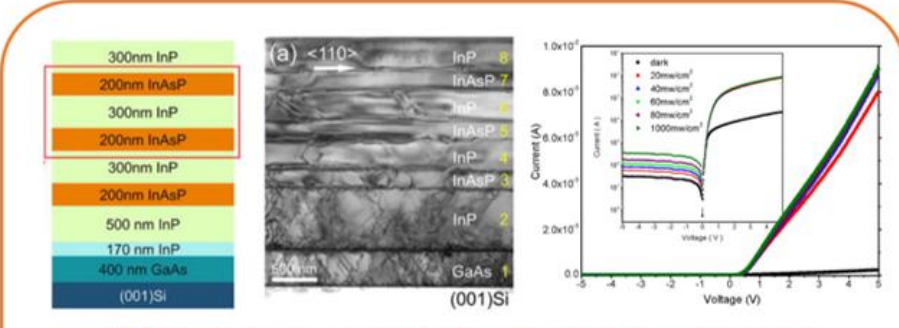


Highlights 2024





WG 2: Applications-oriented material developments



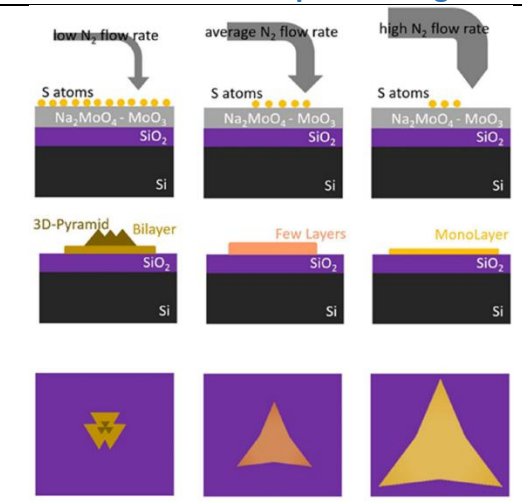
WG 3: Industry-oriented materials development and technological transfers

Table of Contents

-	Fundamental research: new materials (WG1)	1
11-	- Applications- and Industry-oriented material	
de	evelopments (WG2&3)	. 16

I- Fundamental research: new materials (WG1)

Influence of the Carrier Gas Flow in the CVD Synthesis of 2-Dimensional MoS₂ Based on the Spin-Coating of Liquid Molybdenum Precursors



Reference: Nanomaterials, 14(21), 1749. (2024); doi: https://doi.org/10.3390/nano14211749

Authors: F. Esposito, M. Bosi, G. Attolini, F. Rossi, R. Fornari,

F. Fabbri and L. Seravalli

Laboratories: CNR-IMEM (Parma, Italy), University of

Parma (Italy), CNR-NEST (Pisa, Italy)

Techniques: CVD, SEM, OM, Raman Spectroscopy, PL

Spectroscopy

Materials: MoS₂

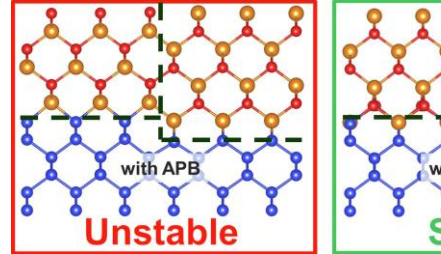
Abstract

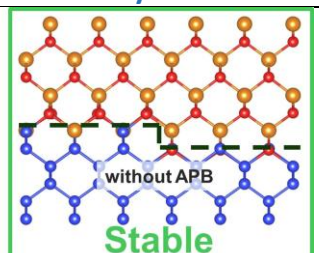
In this work, we study the effects of the carrier gas flow rate on the properties of two-dimensional molybdenum disulfide grown by liquid-precursor-intermediate chemical vapor deposition on SiO₂/Si substrates. We characterized the samples using Optical Microscopy, Scanning Electron Microscopy, spectroscopy, and Photoluminescence spectroscopy. We analyzed samples grown with different nitrogen carrier flows, ranging from 150 to 300 sccm, and discussed the effect of carrier gas flows on their properties. We found a correlation between MoS₂ flake lateral size, shape, and number of layers, and we present a qualitative growth model based on changes in sulfur provision caused by different carrier flows. We show how the use of liquid precursors can allow for the synthesis of homogeneous, single-layer flakes up to 100 μ m in lateral size by optimizing the gas flow rate. These results are essential for gaining a deeper understanding of the growth process of MoS_2 .

OPERA Work Group

WG1

Stability of monodomain III-V crystals and antiphase boundaries over a Si monoatomic step





Reference: Applied Surface Science 678, 161076 (2024);
DOI: https://doi.org/10.1016/j.apsusc.2024.161076

Authors: D. Gupta, S. Pallikkara Chandrasekharan, S.

Thebaud, C. Cornet, and L. Pedesseau. Laboratories: Institut FOTON (Fr).

Techniques: DFT

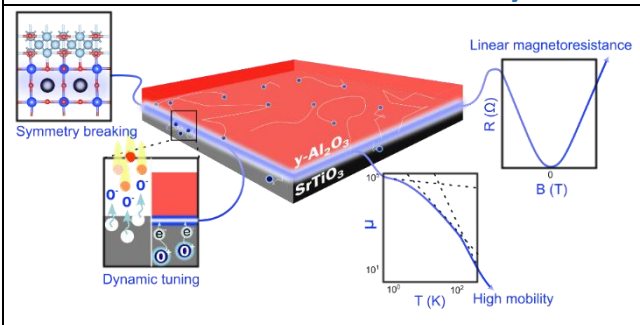
Materials: GaP/Si(001)

Abstract

Here, we compare the stabilities of different III-V crystals configurations on stepped Si substrates, with or without antiphase boundaries, for abrupt and compensated interfaces, using density functional theory. Thermodynamic stability of the different heterostructures is analyzed with an atomic scale description of charge densities distribution and mechanical strain. We show that the configuration where a III-V crystal adapts to a Si monoatomic step through change of charge compensation at the hetero-interface is much more stable than the configuration in which an antiphase boundary is formed. This study thus demonstrates that antiphase boundaries commonly observed in III-V/Si samples are not originating from Si monoatomic step edges but from inevitable kinetically driven coalescence of monophase 3D III-V islands.

OPERA Work Group

Extreme magnetoresistance at high-mobility oxide heterointerfaces with dynamic defect tunability



Reference: Nat Commun 15, 4249 (2024). DOI:

10.1038/s41467-024-48398-8

Authors: D. V. Christensen, T. S. Steegemans, T. D. Pomar, Y. Z. Chen, A. Smith, V. N. Strocov, B. Kalisky & N. Pryds Laboratories: DTU Energy, CAS Beijing, Paul-Scherrer

Institute, Bar-Ilan University

Techniques: PLD, scanning SQUID, magnetotransport,

ARPES

Materials: v-Al₂O₃/SrTiO₃

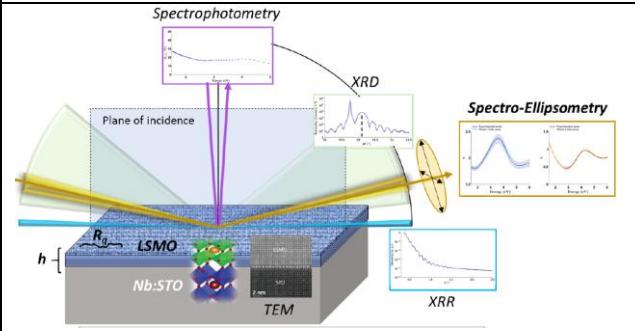
Abstract

Magnetic field-induced changes in the electrical resistance of materials reveal insights into the fundamental properties governing their electronic and magnetic behavior. Various classes of magnetoresistance have been realized, including giant, colossal, and extraordinary magnetoresistance, each with distinct physical origins. In recent years, extreme magnetoresistance (XMR) has been observed in topological and non-topological materials displaying a non-saturating magnetoresistance reaching 10³–10⁸% in magnetic fields up to 60 T. XMR is often intimately linked to a gapless band structure with steep bands and charge compensation. Here, we show that a linear XMR of 80,000% at 15 T and 2 K emerges at the high-mobility interface between the large band-gap oxides y- Al_2O_3 and $SrTiO_3$. Despite the chemically and electronically very dissimilar environment, the temperature/field phase diagrams of γ-Al₂O₃/SrTiO₃ bear a striking resemblance to XMR semimetals. By comparing magnetotransport, microscopic current imaging, and momentum-resolved band structures, we conclude that the XMR in γ-Al₂O₃/SrTiO₃ is not strongly linked to the band structure, but arises from weak disorder enforcing a squeezed guiding center motion of electrons. We also present a dynamic XMR self-enhancement through an autonomous redistribution of quasi-mobile oxygen vacancies. Our findings shed new light on XMR and introduce tunability using dynamic defect engineering.

OPERA Work Group

WG1

Optical constants and thickness determination of La_{2/3}Sr_{1/3}MnO₃ thin films on Nb:SrTiO3 substrates by spectro-ellipsometry: Combination of optical and X-ray techniques



Reference: Applied Surface Science 669 (2024) 160489; doi: 10.1016/j.apsusc.2024.160489.

Authors: J. Blond, C. Dufour, S.K. Chaluvadi, S. Duprey, X. Portier, P. Marie, V. Pierron, L. Méchin, B. Guillet.

Laboratories: GREYC (Fr), CIMAP (Fr), CNR-IOM (It).

Techniques: PLD.

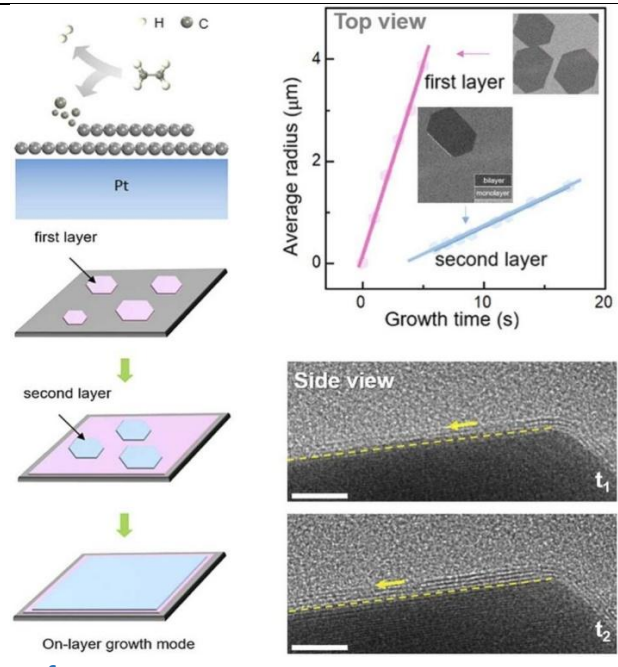
Materials: La_{2/3}Sr_{1/3}MnO₃

Abstract

40 nm thick $La_{2/3}Sr_{1/3}MnO_3$ (LSMO) thin films were epitaxially grown by Pulsed Laser Deposition (PLD) onto niobium doped SrTiO3 (Nb:STO) substrates, with different Nb concentration from 0.01%wt to 0.5%wt. The optical characterization of the heterostructures by spectroscopic ellipsometry enables us to extract the optical constants of the manganite heteroepitaxial layer at room temperature. Performing spectrophotometry in the same wavelength range brings a useful cross-validation of the extracted results. In addition, the thickness evaluation of the LSMO layer by spectro-ellipsometry is further validated by both High Resolution X-ray diffraction and X-ray reflectivity, as well as a Transmission Electron Microscopy cross section, taken as a physical reference. This study validates quantitatively the spectro-ellipsometry as a suitable routine tool to measure accurately both thickness and complex refractive index of the LSMO thin film, picturing their peculiar electrical behaviour between both metallic and insulating phases. The relative error on the thickness measurement between X-ray and ellipsometry is less than 5%. The LSMO complex refractive index enabled also a simultaneous estimation of further material properties, such as the optical gap ω_g or the mass density ρm , determined with less than 1.5% relative error compared to X-ray reflectivity results.

OPERA Work Group

Layer-by-layer growth of bilayer graphene single-crystals enabled by proximity catalytic activity



Reference: Nano Today 59, 102480 (2024); doi; 0.1016/j.nantod.2024.102482

Authors: Z. Zhang, L. Zhou, Z. Chen, A. Jaroš, M. Kolíbal, P. Bábor...Z.-J. Wang.

Laboratories: Ranmin University **(Cn)**, Peking University **(Cn)**, ShanghaiTech **(Cn)**, CEITEC BUT **(Cz)**, Beijing Institute of Technology **(Cn)**, ETH Zurich **(Sui)**

Techniques: CVD, SEM, DFT, LEED, STM, STEM, Raman

Materials: graphene

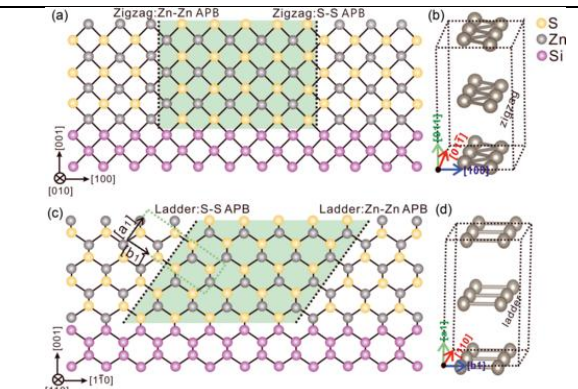
Abstract

Direct growth of large-area vertically stacked two-dimensional (2D) van der Waal (vdW) materials is a prerequisite for their high-end applications in integrated electronics, optoelectronics and photovoltaics. Currently, centimetre- to even metre-scale monolayers of single-crystal graphene (MLG) and hexagonal boron nitride (h-BN) have been achieved by epitaxial growth on various single-crystalline substrates. However, in principle, this success in monolayer epitaxy seems extremely difficult to be replicated to bi- or few-layer growth, as the full coverage of the first layer was believed to terminate the reactivity of those adopting catalytic metal surfaces. Here, we report an exceptional layer-by-layer chemical vapour deposition (CVD) growth of large size bi-layer graphene single-crystals, enabled by proximity catalytic activity from platinum (Pt) surfaces to the outermost graphene layers. In-situ growth and real-time surveillance experiments, under well-controlled environments, unambiguously verify that the growth does follow the layer-bylayer mode on open surfaces of MLG/Pt(111). First-principles calculations indicate that the transmittal of catalytic activity is allowed by an appreciable electronic hybridisation between graphene overlayers and Pt surfaces, enabling catalytic dissociation of hydrocarbons and subsequently direct graphitisation of their radicals on the outermost sp2 carbon surface. This proximity catalytic activity is also proven to be robust for tube-furnace CVD in fabricating single-crystalline graphene bi-, tri- and tetra-layers, as well as h-BN few-layers. Our findings offer an exceptional strategy for potential controllable, layer-by-layer and wafer-scale growth of vertically stacked few-layered 2D single crystals.

OPERA Work Group

WG1

Strain-induced band-to-band Fermi level tuning in II-VI and III-V antiphase boundaries



Reference: Phys. Rev. B 109, 085404 (2024);
DOI: https://doi.org/10.1103/PhysRevB.109.085404
Authors: L. Chen, Z. Chen, J. Zhao, L. Pedesseau, and C. Cornet.

Cornet.

Laboratories: Institut FOTON (Fr), Tianjin Key Laboratory

(Cn).

Techniques: DFT

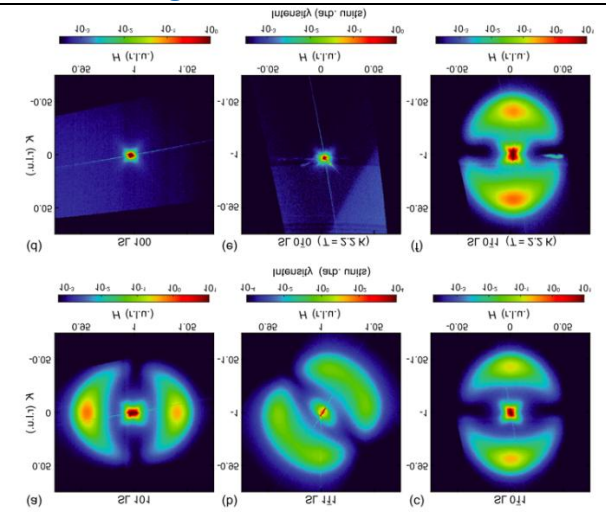
Materials: ZnS/Si(001) and InP/Si(001)

Abstract

Here, we investigate and analyze the electronic properties of ladder- and zigzag-patterned antiphase boundaries (APBs) in II-VI and III-V semiconductors based on first-principles calculations performed on ZnS and InP. From the band-structure analysis on these configurations, we evidence a direct correlation between Fermi levels positioning and the bond length in ladder-patterned APBs. The changes on the APB bond lengths and electronic properties from III-V to II-VI ladder APBs are discussed based on the charges and atoms electronegativity. We then show how the specific atomic configuration of the zigzag-patterned and ladder-patterned APBs differ from the point of view of force accommodation. As a result, ladder-patterned APBs are found to be much more sensitive to any change of stress or the chemical environment. We finally demonstrate that a small change in the APB bond length deeply modifies the band structure and optoelectronic properties of the systems (for both III-V and II-VI semiconductors), with possible n- and p-doping type inversion, thus opening the way towards APB-engineered photoelectric devices.

OPERA Work Group

Assessing the nature of nanoscale ferroelectric domain walls in lead titanate multilayers



Reference: Physical Review X, 14(4), 1–18 (2024). https://doi.org/10.1103/PhysRevX.14.041052

Authors: Zatterin, E., Ondrejkovic, P., Bastogne, L., Lichtensteiger, C., Tovaglieri, L., Chaney, D. A., Sasani, A., Schülli, T., Bosak, A., Leake, S., Zubko, P., Ghosez, P., Hlinka, J., Triscone, J. M., & Hadjimichael, M.

Laboratories: ESRF(Fr), IPCAS(Czech Republic), Q-MAT(Be), UNIGE-DQMP (CH), UCL (UK), LCN (UK), Uni. Warwick (UK)

Techniques: XRD, 1st and 2nd Principles, Phase Field

Materials: PbTiO₃/SrTiO₃ multilayers

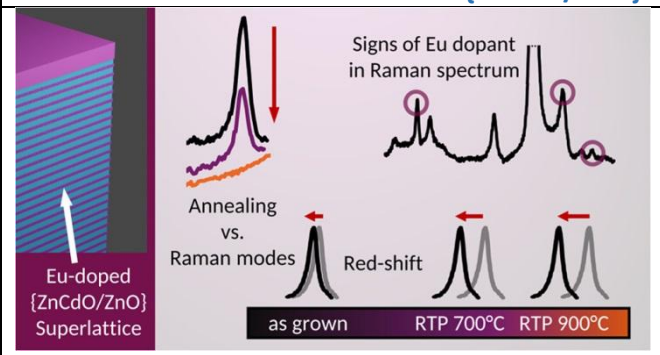
Abstract

The observation of unexpected polarization textures such as vortices, skyrmions, and merons in various oxide heterostructures has challenged the widely accepted picture of ferroelectric domain walls as being Ising-like. Bloch components in the 180° domain walls of $PbTiO_3$ have recently been reported in PbTiO₃/SrTiO₃ superlattices and linked to domain wall chirality. While this opens exciting perspectives, the ubiquity of this Bloch component remains to be further explored. In this work, we present a comprehensive investigation of domain walls in PbTiO₃/SrTiO₃ superlattices, involving a combination of first- and second-principles calculations, phase-field simulations, diffuse scattering calculations, and synchrotron-based diffuse x-ray scattering. Our theoretical calculations highlight that the previously predicted Bloch polarization in the 180° domain walls in PbTiO₃/SrTiO₃ superlattices might be more sensitive to the boundary conditions than initially thought and is not always expected to appear. Employing diffuse scattering calculations for larger systems, we develop a method to probe the complex structure of domain walls in these superlattices via diffuse x-ray scattering measurements. Through this approach, we investigate depolarization-driven ferroelectric polarization rotation at the domain walls. Our experimental findings, consistent with our theoretical predictions for realistic domain periods, do not reveal any signatures of a Bloch component in the centers of the 180° domain walls of PbTiO₃/SrTiO₃ superlattices, suggesting that the precise nature of domain walls in the ultrathin PbTiO₃ layers is more intricate than previously thought and deserves further attention.

OPERA Work Group

WG1

Manifestation of Eu Dopants in Raman Spectra and Doping Concentration Profiles of {ZnCdO/ZnO} Superlattices



Reference: Cryst. Growth Des. 24(16), 6691-6700 (2024); doi: 10.1021/acs.cgd.4c00619.

Authors: I. Perlikowski, E. Zielony, A. Lysak, R. Jakieła and E.

Przeździecka.

Laboratories: Wrocław Tech. (PL), IP PAS (PL).

Techniques: MBE, RRS, C-V profiling, RTP, SEM, SIMS.

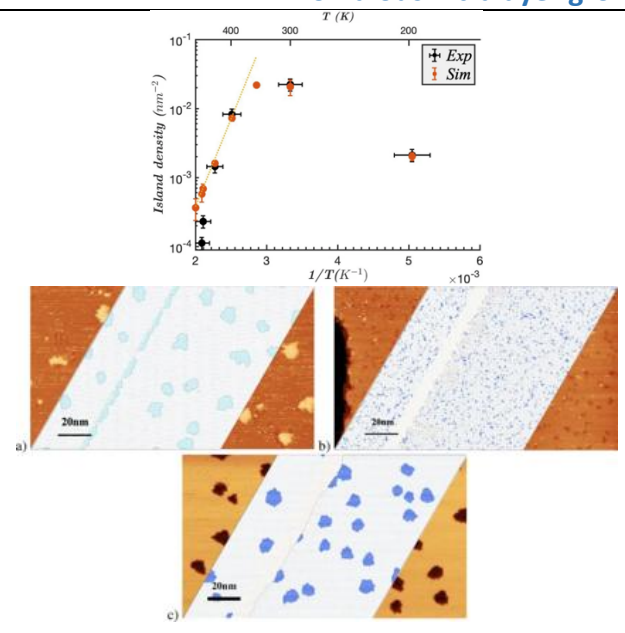
Materials: Eu-doped {ZnCdO/ZnO} superlattices

Abstract

In this study, we explore the effects of europium (Eu) doping {ZnCdO/ZnO} superlattices (SLs) grown using plasma-assisted molecular beam epitaxy. These structures, promising for optoelectronic applications such as thin-film solar cells, photodetectors, and red-light-emitting diodes, exhibit unique properties influenced by doping and fabrication conditions. scattering measurements confirmed incorporation of Eu atoms into the SL, evidenced by the emergence of three forbidden ZnO-related modes, which were absent in bulk ZnO and undoped reference structures. Rapid thermal processing reduced oxygen vacancies and significantly enhanced the crystalline quality, as indicated by the improved ZnO phonon modes. However, annealing also increased tensile strain in the SL due to the incorporation of Cd and Eu into the ZnO host lattice, with changes attributed to oxygen vacancy reduction and atomic rearrangements Current-voltage around Eu ions. measurements demonstrated photocurrent generation capabilities, even under zero external voltage bias, showcasing the photoactivity of the Eu-doped superlattices.

OPERA Work Group

Anomalous intralayer growth of epitaxial Si on Ag(111)



Reference: Scientific Reports | (2024) 14:2401

Doi: 10.1038/s41598-024-52348-1

Authors: K. Wang, G. Prévot and J.-N. Aqua

Laboratories: Institut des NanoSciences de Paris (Fr)

Techniques: Kinetic Monte-Carlo simulation, STM

Materials: Si/Ag(111)

Abstract

The first 2D material, graphene, was discovered in 2004 by exfoliation. It attracted much attention because of its remarkable properties which are different from graphite. However, the limitations of graphene, such as a small band gap, integration challenges, and optical properties, have spurred exploration into alternative 2D materials. Silicene, 2D material of silicon, stands out as a promising candidate. Unlike graphene, silicene lacks a pi-stacking structure, making exfoliation impossible. Epitaxy, known for producing high-quality materials, is thence the only method for silicene synthesis. The epitaxial growth of 2D Si on Ag(111) reveals unexpected growth modes. Instead of forming a silicene lover, silicon grows

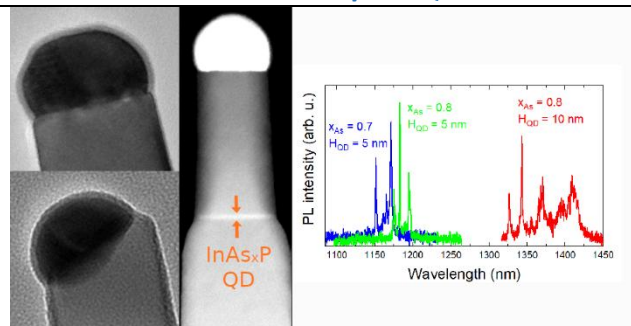
growth modes. Instead of forming a silicene layer, silicon atoms were observed to incorporate into the first atomic layer of the substrate, leading to the formation of inserted islands.

In order to rationalize this anomalous growth behavior, we developed an out-of-equilibrium epitaxial growth model based on kinetic Monte Carlo simulations[2]. The model incorporates several experimentally observed effects, including the energy barrier for intermixing, the barrier associated with the exchange of a Si adatom and a Ag substrate atom, and the distinct interactions between Si and Ag atoms acting parallel and perpendicular to the substrate plane, each governed by different energy barrier parameters. These parameters were parametrized thanks to an approach in which we show that relatively precise estimates of energy barriers can be deduced by meticulous analysis of atomic microscopy images. This detailed approach enables the model to accurately reproduce both qualitatively and quantitatively the anomalous growth patterns of silicon on Ag(111).

OPERA Work Group

WG1

Zincblende InAsxP1-x/InP Quantum Dot Nanowires for Telecom Wavelength Emission



Reference: ACS Appl. Mater. Interfaces 2024, 16, 20, 26491–26499. doi: 10.1021/acsami.4c00615

Authors: G. Bucci, V. Zannier, F. Rossi, A. Musiał, J. Boniecki, G. Sek and L. Sorba

Laboratories: Scuola Normale Superiore di Pisa (It); NEST Istituto Nanoscienze Consiglio Nazionale delle Ricerche (CNR) (It); Istituto dei Materiali per l'Elettronica ed il Magnerismo (IMEM) – Consiglio Nazionale delle Ricerche (CNR) (It); Department of Experimental Physics, Wrocław University of Science and Technology (PI)

Techniques: CBE, TEM, μ-PL

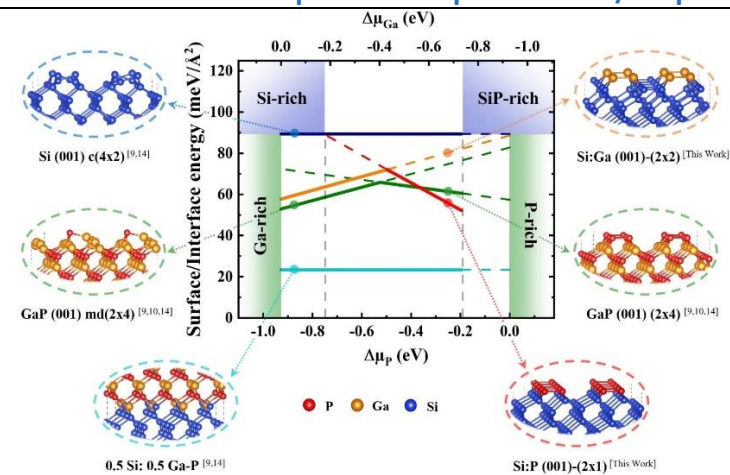
Materials: $InAs_xP_{1-x}$ quantum dots in InP nanowires

Abstract

InAs_xP_{1-x} quantum dots (QDs) in InP nanowires (NWs) have been realized as a platform for emission at telecom wavelengths. These QDs are typically grown in NWs with the wurtzite crystal phase, but in this case, ultrathin diameters are required to achieve defect-free heterostructures, making the structures less robust. In this work, we demonstrate the growth of pure zincblende InAs_xP_{1-x} QDs in InP NWs, which enabled an increase in NW diameters to about 45 nm, achieved by employing Au-assisted vapor liquid solid growth in a chemical beam epitaxy system. We studied the growth of InP/ $InAs_xP_{1-x}$ heterostructures with different compositions to control the straight growth along the (100) direction and to tune the emission wavelength. Interestingly, we found that the growth mechanism for pure InAs QDs is different compared to that for $InAs_xP_{1-x}$ alloy QDs. This allowed us to optimize different growth protocols to achieve straight growth of the final QD NWs. We successfully obtained growth of $InAs_xP_{1-x}$ QDs with a composition in the range of x = 0.24-1.00. By means of low temperature microphotoluminescence measurements, we demonstrate the tunability of the emission in the broad near infrared spectral range from 1120 to 1430 nm, in dependence of the $InAs_xP_{1-x}$ QD composition and morphology, remarkably observing an emission at the telecom O-band for a 10 nm thick QD with 80% of As content.

OPERA Work Group

Inevitable Si surface passivation prior to III-V/Si epitaxy: Strong impact on wetting properties



Reference: Phys. Rev. B 109, 045304 (2024); DOI: https://doi.org/10.1103/PhysRevB.109.045304

Authors: S. Pallikkara Chandrasekharan, D. Gupta, C. Cornet, and L.

Pedesseau.

Laboratories: Institut FOTON (Fr).

Techniques: DFT
Materials: GaP/Si(001)

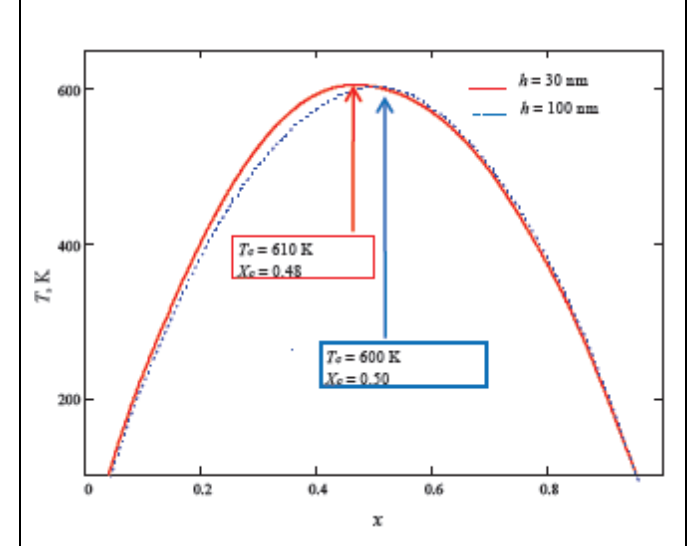
Abstract

Here, we quantitatively estimate the impact of the inevitable Si surface passivation prior to III-V/Si heteroepitaxy on the surface energy of the Si initial substrate, and explore its consequences for the description of wetting properties. Density functional theory is used to determine absolute surface energies of P- and Ga-passivated Si surfaces and their dependences with the chemical potential. Especially, we show that, while a ≈90meV/Å² surface energy is usually considered for the nude Si surface, surface passivation by Ga- or P- atoms leads to a strong stabilization of the surface, with a surface energy in the [50–75 meV/Å²] range. The all ab initio analysis of the wetting properties indicate that a complete wetting situation would become possible only if the initial passivated Si surface could be destabilized by at least 15meV/Å² or if the III-V (001) surface could be stabilized by the same amount.

OPERA Work Group

WG1

Phase Stability of ZnSb-SnTe Thin Films with High Thermoelectric Performance



Reference: 2024 IEEE 42nd Int. Conf. Electronics and Nanotechnology (ELNANO), Kyiv, Ukraine, 2024, 211-214; DOI: 10.1109/ELNANO63394.2024.10756846

Authors: V. Deibuk.

Laboratories: Chernivtsi National University (Ua).

Techniques: Theory .

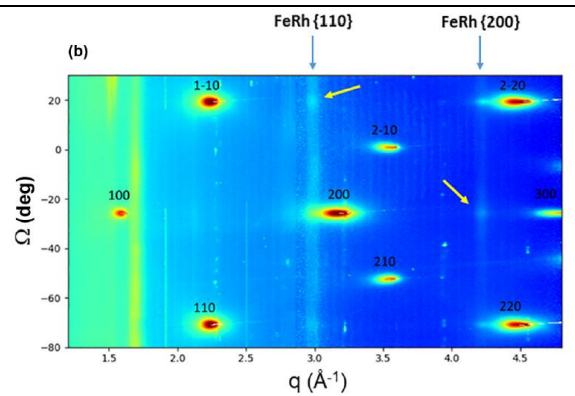
Materials: ZnSb-SnTe/SiO₂

Abstract

the search for flexible thermoelectric materials with high figure of merit is currently an urgent task. The article theoretically studies the phase stability of thin films of pseudobinary semiconductor alloys ZnSb-SnTe. The obtained T-x phase diagrams made it possible to predict the existence of a wide miscibility gap. Taking into account small internal stresses and the influence of the quartz substrate did not lead to significant changes in the phase diagram depending on the film thickness. It has been shown that spinodal decomposition processes caused by annealing at T=225°C in $(ZnSb)_{1-x}(SnTe)_x/SiO_2$ thin films at x=0.27 lead to microstructural evolution with the formation of precipitates of the SnSb metal phase. This fact is in good agreement with the experimental studies of the thin films considered and is the reason for the sharp increase in the power factor to 3383 μWm⁻¹K⁻¹ at 300°C. The described recrystallization processes are the main mechanism for the high thermoelectric characteristics of this material.

OPERA Work Group

Preferential orientations of FeRh nanomagnets deposited on a BaTiO3 epitaxial thin film



Reference: Phys. Rev. B 109, 245410 (2024);

doi: 10.1103/PhysRevB.109.245410.

Authors: A. Reyes, G. Herrera, P. Capiod, D. Le Roy, V. Dupuis, I. Cañero-Infante, G. Saint-Girons, R. Bachelet, A. Resta, P. Ohresser, L. Martinelli, X. Weng, G. Renaud and F. Tournus Laboratories: ILM, INL, SOLEIL, Institut Néel, CEA Grenoble

Techniques: LECBD, MBE, PLD, GISAXS, XRD, XMCD.

Materials: FeRh on BaTiO₃, SrTiO₃

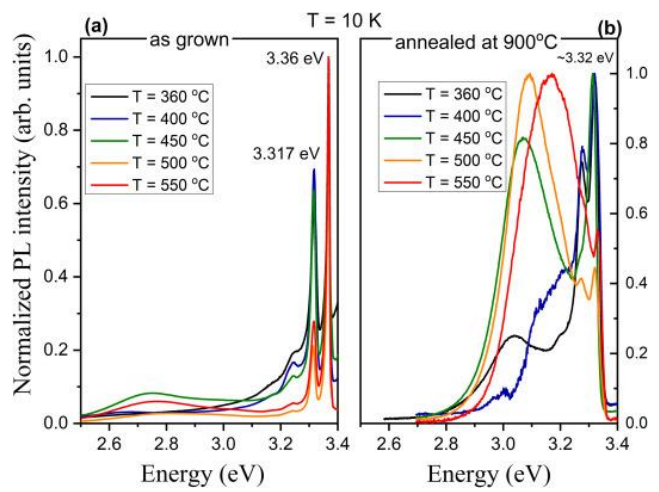
Abstract

Size-selected FeRh clusters have been deposited at low energy and under ultra-high vacuum conditions, on a BaTiO₃ epitaxial thin film. Using x-ray diffraction in grazing incidence configuration, we have observed the chemical ordering of FeRh nanoparticles into the chemically ordered B2 phase after annealing, while a reciprocal space mapping indicates that particles, despite their random deposition, are finally adopting preferential orientations reflecting an atomic ordering with the BaTiO3 crystal. In addition to the usual epitaxy relationship observed for FeRh thin films, an unexpected orientation is detected (45° in-plane rotation, leading to a new cube-on-cube epitaxy relationship), which must be specific to nanosized FeRh particles.

OPERA Work Group

WG1

Influence of the growth temperature and annealing on the optical properties of {CdO/ZnO}₃₀ superlattices



Reference: J. Lumin. 269,120481 (2024);

doi: 10.1016/j.jlumin.2024.120481.

Authors: E. Przeździecka, A. Lysak, A. Adhikari, M. Stachowicz, A. Wierzbicka, R. Jakiela, Z. Khosravizadeh, P. Sybilski, A. Kozanecki.

Laboratories: IP PAS (PL).

Techniques: MBE, XRD, RTP, SIMS, PL, UV-Vis

spectrophotometry.

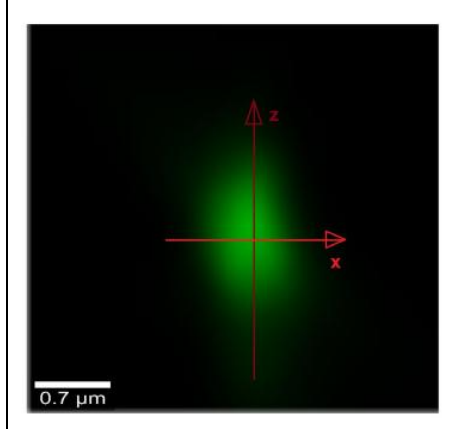
Materials: {ZnO/CdO} superlattices

Abstract

In this work, we investigated the optical properties of shortperiod {CdO/ZnO} superlattices (SLs) grown by plasmaassisted molecular beam epitaxy. SL structures were successfully deposited at temperatures from 360 to 550°C. Our study reveals the significant impact of growth temperature on the crystallographic and optical qualities of these structures. X-ray diffraction (XRD) and secondary ion mass spectrometry (SIMS) analyses confirm that lower growth temperatures yield higher crystal quality, with well-Luminescence studies defined superlattice periodicity. indicated that UV emission dominates in as-grown SLs. Rapid thermal annealing (RTA) at 900°C introduced significant changes in the optical properties of the samples. NBE emission peaks broadened and redshifted to lower energies, while intense defect-related luminescence bands emerged, with their intensities and spectral positions strongly dependent on growth temperature. These effects are attributed to interdiffusion of Zn and Cd atoms during annealing, leading to partial or complete degradation of the SL structure. Lower growth temperatures yielded SLs that were more resistant to high-temperature annealing and exhibited less intense defect-related luminescence. These findings provide insights into optimizing growth and posttreatment processes for potential applications in optoelectronic devices based on {CdO/ZnO} SLs.

OPERA Work Group

Visualization and Estimation of 0D to 1D Nanostructure Size by Photoluminescence



Reference: Nanomaterials 2024, 14, 1988. https://doi.org/10.3390/nano14241988

Authors: A. Medvids, A. Pludons, A. Vaitkevicius, S.

Miasojedovas and P. Ščajev*

Laboratories: RTU(LV), VU(LT)

Techniques: SNOM, PL

Materials: DLC, Si nanostructures

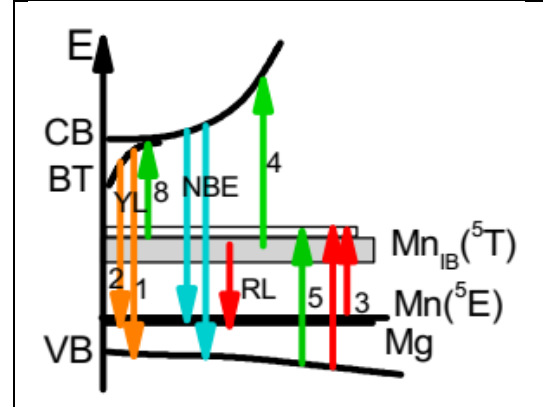
Abstract

We elaborate a method for determining the OD-1D nanostructure size by photoluminescence (PL) emission spectrum dependence on the nanostructure dimensions. As observed, the high number of diamond-like carbon nanocones shows a strongly blue-shifted PL spectrum compared to the bulk material, allowing for the calculation of their top dimensions of 2.0 nm. For the second structure model, we used a sharp atomic force microscope (AFM) tip, which showed green emission localized on its top, as determined by confocal microscopy. Using the PL spectrum, the calculation allowed us to determine the tip size of 1.5 nm, which correlated well with the SEM measurements. The time resolved PL measurements shed light on the recombination process, providing stretched-exponent decay with a $\tau 0 = 1$ ns lifetime, indicating a gradual decrease in exciton lifetime along the height of the cone from the base to the top due to surface and radiative recombination. Therefore, the proposed method provides a simple optical procedure for determining an AFM tip or other nanocone structure sharpness without the need for sample preparation and special expensive equipment.

OPERA Work Group

WG1

Photo-Excited Carrier Dynamics in Ammonothermal Mn-Compensated GaN Semiconductor



Reference: Materials 2024, 17, 5995. https://doi.org/10.3390/ma17235995

Authors: Patrik Ščajev*, Paweł Prystawko, Robert Kucharski

and Irmantas Kašalynas

Laboratories: UNIPRESS(PL), FTMC(LT), VU(LT)
Techniques: MOCVD, ammonothermal method, PL

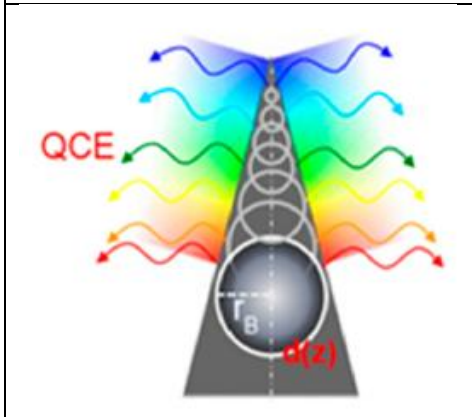
Materials: GaN semiconductor

Abstract

We investigated the carrier dynamics of ammonothermal Mncompensated gallium nitride (GaN:Mn) semiconductors by using sub-bandgap and above-bandgap photo-excitation in a photoluminescence analysis and pump-probe measurements. The contactless probing methods elucidated their versatility for the complex analysis of defects in GaN:Mn crystals. The impurities of Mn were found to show photoconductivity and absorption bands starting at the 700 nm wavelength threshold and a broad peak located at 800 nm. Here, we determined the impact of Mn-induced states and Mgacceptors on the relaxation rates of charge carriers in GaN:Mn based on a photoluminescence analysis and pump-probe measurements. The electrons in the conduction band tails were found to be responsible for both the photoconductivity and yellow luminescence decays. The yellow photoluminescence decays exhibited a 1 ns decay time at low laser excitations, whereas, at the highest ones, it increased up to 7 ns due to the saturation of the nonradiative defects, resembling the photoconductivity lifetime dependence. The fast photo-carrier decay time observed in ammonothermal GaN:Mn is of critical importance in high-frequency and high-voltage device applications.

OPERA Work Group

Quantum Cone—A Nano-Source of Light with Dispersive Spectrum Distributed along Height and in Time



Reference: Nanomaterials 2024, 14, 1580. https://doi.org/10.3390/nano14191580
Authors: A. Medvids, P. Ščajev and K. Hara Laboratories: SU(JP), RTU(LV), VU(LT)
Techniques: magnetron sputtering, PL.

Materials: DLC layers and nanocones

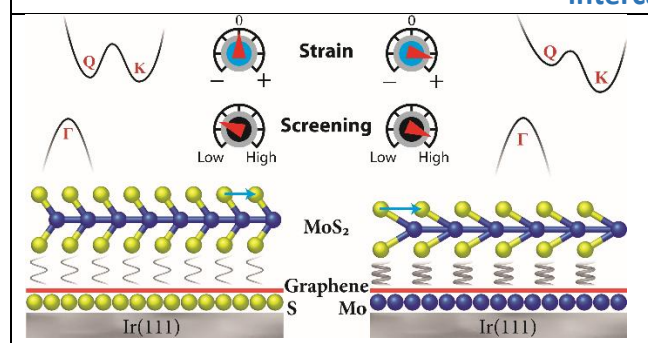
Abstract

We study a quantum cone, a novel structure composed of multiple quantum dots with gradually decreasing diameters from the base to the top. The dot distribution leads to a dispersive radiated spectrum. The blue edge of the spectrum is determined by the quantum confinement of excitons on top of the cones, while the red edge is determined by the bandgap of a semiconductor. We observe the kinetics of photoluminescence by obeying the stretch-exponential law from quantum cones formed on the surface of diamond-like carbon (DLC). They are explained by an increase in the lifetime of excitons along the height of the cone from the top to the base of the cone and an increasing concentration of excitons at the base due to their drift in the quasi-built-in electric field of the quantum cone. The possible visualization of the quantum cone tops of DLC using irradiation by a UV light source is shown. A quantum cone is an innovative nano-source of light because it substitutes for two elements in a conventional spectrometer: a source of light and a dispersive element—an ultrafast monochromator. These features enable the building of a nano-spectrometer to measure the absorbance spectra of virus and molecule particles.

OPERA Work Group

WG1

Probing the interplay of interactions, screening and strain in monolayer MoS2 via selfintercalation



Reference: npj 2D Mater Appl 8, 61 (2024);

DOI:10.1038/s41699-024-00488-3

Authors: B. Pielić, M. Mužević, D. Novko, J. Cai, A. Bremerich, R. Ohmann, M. Kralj, I. Šrut Rakić & C. Busse

Laboratories: SiMAT, Institute of physics (HR), Lestkörperphysik, Univ. Siegen (DE)

Techniques: MBE, STM, STS, DFT

Materials: intercalated single layer MoS₂,

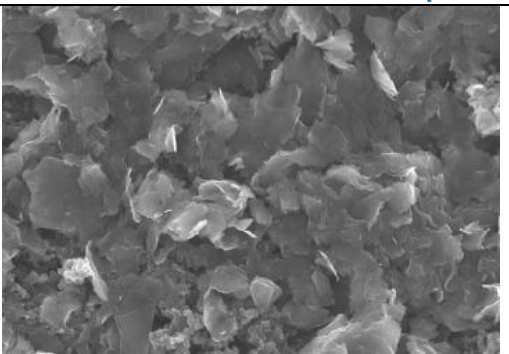
MoS₂/graphene/Ir(111)

Abstract

Controlling many-body interactions in two-dimensional systems remains a formidable task from the perspective of both fundamental physics and application. Here, we explore remarkable electronic structure alterations of MoS2 monolayer islands on graphene on Ir(111) induced by non-invasive self-intercalation. This introduces significant differences in morphology and strain of MoS2 as a result of the modified interaction with the substrate. Consequently, considerable changes of the band gap and non-rigid electronic shifts of valleys are detected, which are a combined effect of the screening of the many-body interactions and strain in MoS2. Furthermore, theory shows that each substrate leaves a unique stamp on the electronic structure of two-dimensional material in terms of those two parameters, restricted by their correlation.

OPERA Work Group

Oxidized Graphite Nanocrystals for White Light Emission



Reference: Crystals 2024, 14, 505. https://doi.org/10.3390/cryst14060505

Authors: P. Ščajev, S. Miasojedovas, A. Mekys, G. Kreiza,

J. Ceponkus,

V. Šablinskas, T. Malinauskas* and A. Medvids

Laboratories: RTU(LV), VU(LT)

Techniques: spray coating, thermal anneal, Raman,

AFM, SEM, PL

Materials: graphite layers

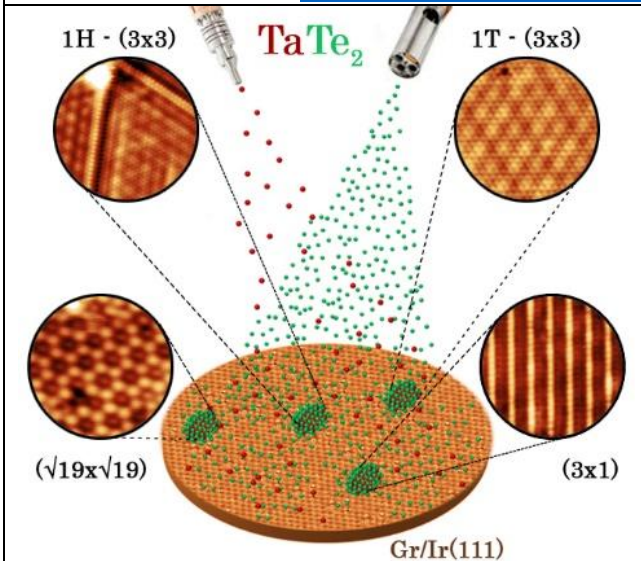
Abstract

We investigated the formation of graphite nanocrystals covered with graphite oxide for white light generation. The nanoparticles were formed using cost-efficient oxidation of a carbon-based dye pigment at different temperatures and verified using X-ray diffraction and Raman measurements. Formation of the graphite nanoparticles via thermal annealing was observed, while their light emission increased at higher oxidation temperatures. This was associated with a higher amount of oxygen defect groups. The timeresolved photoluminescence measurements showed linearly faster decays at shorter wavelengths and similar decays at different annealing temperatures. Broadband and linear vs. excitation emission spectra of the particles were found to be suitable for white-light emitting devices and phosphor markers. The fast photoluminescence decay opens the possibility the application of nanoparticles in optical wireless communication technology

OPERA Work Group

WG1

Metastable Polymorphic Phases in Monolayer TaTe₂



Reference: Small 19, 2300262 (2023); https://doi.org/10.1002/smll.202300262

Authors: I. Di Bernardo, J.Ripoll-Sau, J. Angel Silva-Guillén, F. Calleja, C. G. Ayani, R. Miranda, E. Canadell, M. Garnica, A. L.

Vázquez de Parga

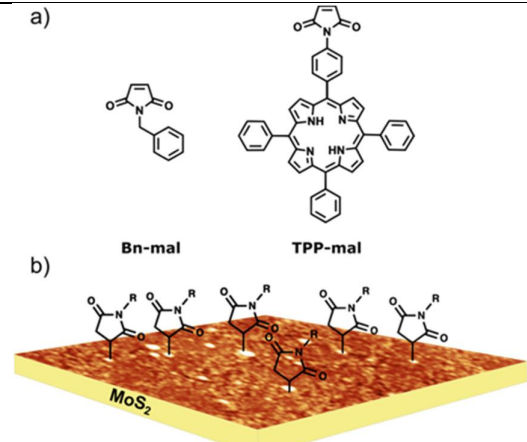
Laboratories: IMDEA Nanoscience Techniques: MBE, STM, DFT Materials: TMDCs, TaTe2

Abstract

Polymorphic phases and collective phenomena—such as charge density waves (CDWs)—in transition metal dichalcogenides (TMDs) dictate the physical and electronic properties of the material. Most TMDs naturally occur in a single given phase, but the fine-tuning of growth conditions via methods such as molecular beam epitaxy (MBE) allows to unlock otherwise inaccessible polymorphic structures. Exploring understanding the morphological and electronic properties of new phases of TMDs is an essential step to enable their exploitation in technological applications. Here, scanning tunneling microscopy (STM) is used to map MBE-grown monolayer (ML) TaTe2. This work reports the first observation of the 1H polymorphic phase, coexisting with the 1T, and demonstrates that their relative coverage can be controlled by adjusting synthesis parameters. Several superperiodic structures, compatible with CDWs, are observed to coexist on the 1T phase. Finally, this work provides theoretical insight on the delicate balance between Te...Te and Ta-Ta interactions that dictates the stability of the different phases. The findings demonstrate that TaTe2 is an ideal platform to investigate competing interactions, and indicate that accurate tuning of growth conditions is key to accessing metastable states in TMDs.

OPERA Work Group

Clicking beyond suspensions: understanding thiol-ene chemistry on solid-supported MoS₂



Reference: Nanoscale 16, 3749 (2024); https://doi.org/10.1039/d3nr05236b

Authors: M. C Rodríguez González, I. M Ibarburu, C. Rebanal, M. Vázquez Sulleiro, R. Sasikumar, A. Naranjo, C. G Ayani, M. Garnica, F. Calleja, E. M

Pérez, A. L Vázquez de Parga, S. De Feyter

Laboratories: IMDEA Nanoscience, Instituto de Materiales y

Nanotecnología, KU Leuven Techniques: MBE, STM, DFT Materials: STM, AFM, Raman

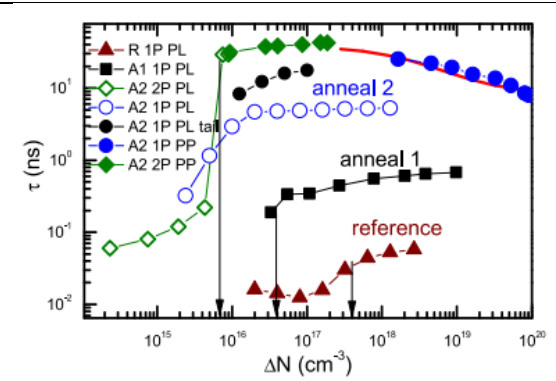
Abstract

Molecular functionalization of MoS_2 has attracted a lot of attention due to its potential to afford finetuned hybrid materials that benefit from the power of synthetic chemistry and molecular design. Here, we report on the on-surface reaction of maleimides on bulk and molecular beam epitaxy grown single-layer MoS_2 , both in ambient conditions as well as ultrahigh vacuum using scanning probe microscopy.

OPERA Work Group

WG1

Long-lived excitons in thermally annealed hydrothermal ZnO



Reference: Heliyon 10 (2024) e26049, https://doi.org/10.1016/j.heliyon.2024.e26049

Authors: P. Ščajev, D. Gogova

Laboratories: VU(LT), BAS (BG), DF(SV)
Techniques: hydrothermal synthesis, thermal

anneal, PL

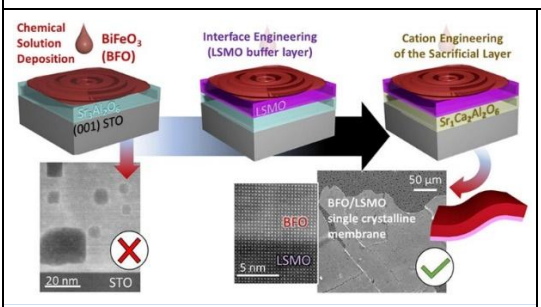
Materials: hydrothermal ZnO

Abstract

Applying thermal annealing to hydrothermal ZnO crystals an enhancement of exciton lifetime from 80 ps to 40 ns was achieved boosting PL quantum efficiency of the UV luminescence up to 70 %. The lifetime improvement is related to the reduced density of carrier traps by a few orders of magnitude as revealed by the reduction of the slow decay tail in pump probe decays coupled with weaker defects-related PL. The diffusion coefficient was determined to be 0.5 cm large exciton diffusion length of 1.4 μ m. The UV PL lifetime drop at the lowest exciton densities was explained by capture to traps. Release of holes from acceptor traps provided delayed exciton luminescence with ~200 μs day time and 390 meV thermal activation energy. Pump-probe decays provided exciton absorption cross-section of 9 × 10-18 cm2 at 1550 nm wavelength and verified the PL decay times of excitons. Amplitudes and decay times of the microsecond slow decay tails have been correlated with the trap densities and their photoluminescence. A surface recombination velocity of 500 cm/s and the bimolecular free carrier recombination coefficient 0.7×10 cm3/s were calculated. Therefore, the properly annealed hydrothermally grown ZnO can be a viable and integral part of many functional devices as light-emitting diodes and lasers.

OPERA Work Group

Unfolding the Challenges To Prepare Single Crystalline Complex Oxide Membranes by Solution Processing



Reference: ACS Appl. Mater. Interfaces 2024, 16, 28, 36796-36803,

https://doi.org/10.1021/acsami.4c05013

Authors: P. Salles, R. Guzman, H. Tan, M. Ramis, I. Fina, P. Machado, F. Sanchez, G. De Luca, W. Zhou, M. Coll

Laboratories: ICMAB-CSIC (Spain), UCAS (China)

Techniques: CSD, PLD, XRD, STEM, EELS, SEM, PFM

Materials: BiFeO₃, La_{0.7}Sr_{0.3}MnO₃, Sr_{3-x}Ca_xAl₂O₆

Abstract

In this work, we presented solution processing, also named chemical solution deposition (CSD), as a cost-effective alternative deposition technique to prepare freestanding membranes identifying the main processing challenges and how to overcome them. In particular, we compared three different strategies based on interface and cation engineering to prepare CSD (00I)-oriented BiFeO3 (BFO) membranes.

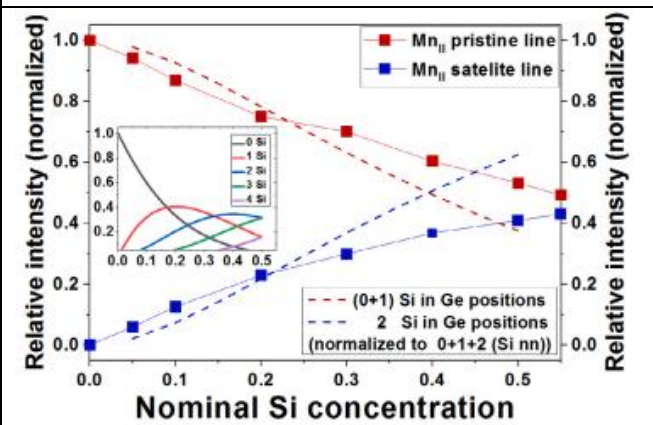
- First, BFO is deposited directly on SAO but forms a nanocomposite of Sr–Al–O rich nanoparticles embedded in an epitaxial BFO matrix because the Sr–O bonds react with the solvents of the BFO precursor solution.
- Second, the incorporation of a pulsed laser deposited La0.7Sr0.3MnO3 (LSMO) buffer layer on SAO prior to the BFO deposition prevents the massive interface reaction and subsequent formation of a nanocomposite but migration of cations from the upper layers to SAO occurs, making the sacrificial layer insoluble in water and withholding the membrane release.
- Finally, in the third scenario, a combination of LSMO with a more robust sacrificial layer composition, SrCa2Al2O6 (SC2AO), offers an ideal building block to obtain (001)-oriented BFO/LSMO bilayer membranes with a high-quality interface that can be successfully transferred to both flexible and rigid host substrates. Ferroelectric fingerprints are identified in the BFO film prior and after membrane release.

These results show the feasibility to use CSD as alternative deposition technique to prepare single crystalline complex oxide membranes widening the range of available phases and functionalities for next-generation electronic devices.

OPERA Work Group

WG1

Magnetic interactions in epitaxial films of Mn₅(Ge_{1-x}Si_x)₃/Ge(111): ⁵⁵Mn NMR study



Reference: J. Magn. Magn. Mater. **600** 172120 (2024);

Doi: 10.1016/j.jmmm.2024.172120

Authors: R. Kalvig, E. Jedryka, S. Kang, M. Petit, L. Michez and

M. Wójcik

Laboratories: Institute of Physics, Polish Academy of Sciences (PL), Aix-Marseille Univ, CNRS, CINAM (FR)

Techniques: NMR, MBE

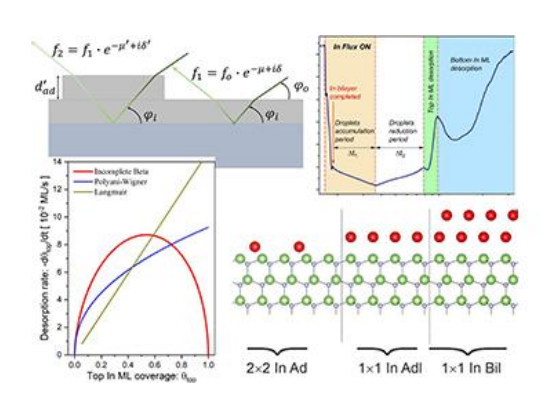
Materials: MBE grown epitaxial thin films of Mn₅(Ge_{1-x}Si_x)₃

Abstract

In this work, using the frequency of ⁵⁵Mn NMR lines as fingerprints of specific magnetic environments we have identified a new population of the 6(g) manganese sites distinguished by a lower magnetic moment, that coexist with the unaltered Mn environments. This effect is attributed to the orbital overlay due to a lattice distortion introduced by Si. Interestingly, these modified Mn sites retain the orbital moment practically unaltered. We show that the number of the new Mn environments for a given concentration coincides with a probability of finding two Si atoms instead of Ge in the nearest neighborhood of a 6(g) site. The effects of Ge replacement with Si in the Mn₅(GeSi)₃ epitaxial films can be regarded as a first step towards creating a low-temperature AFM1 structure reported in Mn₅Si₃ thin films.

OPERA Work Group

Desorption kinetics of indium adlayers on GaN(0001): Fractional order and nonmonotonic behavior



Reference: J. Appl. Phys 136, 215701 (2024); doi; https://doi.org/10.1063/5.0240751

Authors: L. Lymperakis, K. Lymperakis and E. Iliopoulos

Laboratories: Univ. Crete (GR), IESL-FORTH (GR)

Techniques: MBE, RHEED, DFT, quasi-continuous models

Materials: III-N semiconductors

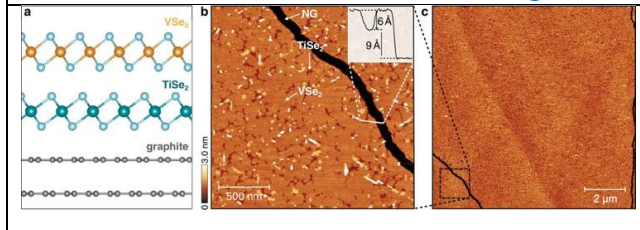
Abstract

Epitaxial growth is a dynamic process and, to first order, is governed by the nature and the rates of elementary surface kinetic mechanisms, such as adatom desorption. In compound type growing surfaces, particularly in III-Nitride molecular beam epitaxy, where the presence of a metallic surface bilayer has a catalytic role, desorption also affects the rates of other elementary mechanisms. In this study, we investigated the desorption of an indium adlayer from GaN(0001) surfaces, a critical kinetic process in the epitaxy of In-containing alloys, using reflection high-energy electron diffraction, density functional theory calculations and quasi-continuous modeling methods to reveal the underlying physical mechanisms. Our results demonstrate that while the indium bilayer desorbs in a layer-by-layer mode, the desorption mechanisms from the bottom and top monolayers differ significantly. The bottom follows a 3/4 order Polyani-Wigner relation, attributed to contributions from two different adlayer phases. The top monolayer desorption exhibits a non-monotonic dependence on coverage. This is associated with the liquidus status of this monolayer and its continuous restructuring during desorption. These findings clarify and quantify indium desorption processes from GaN(0001) surfaces, offering insights into analogous mechanisms in other compound-type material systems.

OPERA Work Group

WG1

Epitaxial Growth of Large-Area Monolayers and van der Waals Heterostructures of Transition-Metal Chalcogenides via Assisted Nucleation



Reference: Advanced Materials 36, 2402254 (2024); DOI: 10.1002/adma.202402254

Authors: A. Rajan, S. Buchberger, B. Edwards, A. Zivanovic, N. Kushwaha, C. Bigi, Y. Nanao, B.K. Saika, O.R. Armitage, P. Wahl, P. Couture, and P.D.C. King.

Laboratories: Univ. St Andrews (UK), MPICPS (DE), STFC

CLS (UK), Univ. Bonn (DE), Univ. Surrey (UK)

Techniques: MBE, AFM, ARPES, XPS, STM, RBS, PIXE Materials: 2D Transition Metal Chalcogenide monolayers (TiSe₂, VSe₂, NbSe₂, Cr₂Te₃, Cr₂Se₃) and heterostructures

(Graphite/TiSe₂/VSe₂)

Abstract

This work addressed key challenges in the scalable fabrication of high-quality transition-metal chalcogenide heterostructures using molecular-beam epitaxy (MBE). Conventional MBE growth of such 2D materials is often limited by non-uniform coverage, poor morphology, and rotational disorder. We demonstrated that introducing a sacrificial species via electronbeam evaporation significantly enhances nucleation, enabling the growth of large-area, uniform monolayers with improved quasiparticle lifetimes. This approach facilitates the synthesis of high-quality epitaxial van der Waals heterostructures by MBE, advancing the potential for scalable 2D material integration.

OPERA Work Group

Surface Charge: An Advantage for the Piezoelectric Properties of GaN Nanowires



Reference: Nanoenergy Adv. 4, 133–146 (2024); doi.org/10.3390/nanoenergyadv4020008

Authors: T. K. Sodhi, P. Chrétien, Q. C. Bui, A. Chevillard, L. Travers, M. Morassi, M. Tchernycheva, F. Houzé, N. Gogneau

Laboratories: Centre de Nanosciences et

Nanotechnologies, Université Paris-Saclay (Fr) ; Laboratoire de Génie Electrique de Paris, CNRS, CentraleSupélec, Université Paris-Saclay (Fr)

Techniques: MBE, AFM
Materials: GaN nanowires

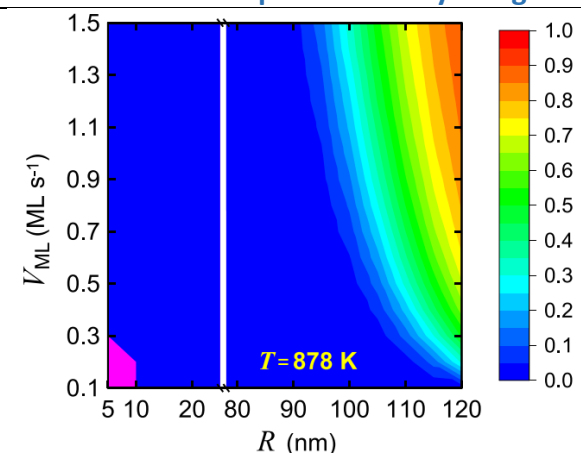
Abstract

The optimization of the new generation of piezoelectric nanogenerators based on 1D nanostructures requires a fundamental understanding of the different physical mechanisms at play, especially those that become predominant at the nanoscale regime. One such phenomenon is the surface charge effect (SCE), which is very pronounced in GaN NWs with sub-100 nm diameters. With an advanced nanocharacterization tool derived from AFM, the influence of SCE on the piezo generation capacity of GaN NWs is investigated by modifying their immediate environment. As-grown GaN NWs are analysed and compared to their post-treated counterparts featuring an Al_2O_3 shell. We establish that the output voltages systematically decrease by the Al₂O₃ shell. This phenomenon is directly related to the decrease of the surface trap density in the presence of Al₂O₃ and the corresponding reduction of the surface Fermi level pinning. This leads to a stronger screening of the piezoelectric charges by the free carriers. These experimental results demonstrate and confirm that the piezoconversion capacity of GaN NWs is favoured by the presence of the surface charges.

OPERA Work Group

WG1

Incomplete monolayer regime and mixed regime of nanowire growth



Reference: Physical Review Materials **8**, 043401 (2024) doi 10.1103/PhysRevMaterials.8.043401

Authors: F. Glas

Laboratories: C2N (Fr)

Techniques: Growth modeling (numerical and analytical)

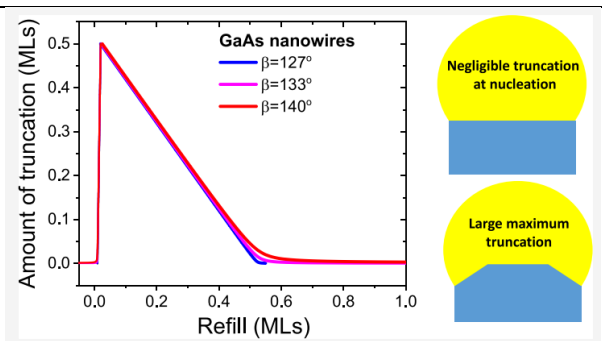
Materials: Nanowires of III-V semiconductors

Abstract

We study theoretically the nucleation and development of sequences of monolayers during the vapor-liquid-solid growth of semiconductor nanowires, in the case where all material originates from the catalyst nanodroplet. If at nucleation the droplet content is insufficient, a fractional monolayer forms quickly before propagating more slowly; the droplet then refills during a random waiting time until next nucleation. We compare the proper incomplete monolayer regime, where this occurs for each monolayer, with the mixed regime where full or fractional monolayers may form, depending on the nucleation event. We investigate in detail the most general case of the mixed regime at arbitrary temperature. Under simple assumptions of the dependence of nucleation and desorption rates upon liquid state, valid at least for III-V compounds (with low concentration of the volatile group V atoms in the liquid), we calculate semianalytically the probability density of the concentration at nucleation and the statistics of the propagation, waiting and monolayer cycle times, without any growth simulation and duly accounting for the correlations between successive monolayers. We find that an effective incomplete monolayer regime, whereby a huge fraction of nucleations produce incomplete monolayers, may prevail over a wide range of nanowire-droplet geometry and growth conditions, with complete monolayers becoming frequent only at large nanowire radius, input rate, and temperature. We explain why, in this regime, growth tends to become quasideterministic, with a very narrow distribution of monolayer cycle times, which is beneficial for a precise control of nanowire ensembles and heterostructures. We investigate quantitatively the case of self-catalyzed GaAs nanowires and discuss the extension of our conclusions to other systems.

OPERA Work Group

Oscillations of truncation in vapor-liquid-solid nanowires



Reference: Crystal Growth & Design 24, 9660-9672 (2024)

doi 10.1021/acs.cgd.4c01162

Authors: V. G. Dubrovskii, F. Glas

Laboratories: Saint Petersburg State University (Russia),

C2N (Fr)

Techniques: Growth modeling (numerical and analytical)

Materials: Nanowires of III-V and elemental

semiconductors

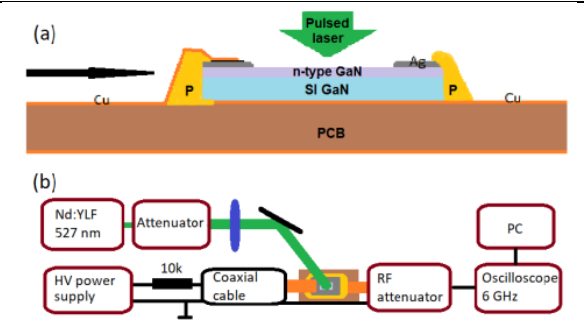
Abstract

The truncated geometry of the liquid-solid interface in Si, Ge, and zinc blende III-V nanowires grown by the vaporliquid-solid method has far-reaching implications in the nanowire morphology, crystal phase, and doping process. It has previously been found that the amount of truncation oscillates insynchronization with the monolayer growth cycle, which was explained within a model of Tersoff and coauthors. Here, we develop an advanced model for the oscillations of the truncated geometry in vapor-liquid-solid nanowires and study in detail different stages of monolayer growth in nanowires with such a geometry. It is shown that the large truncated volumes (on the order of one monolayer) observed experimentally in different nanowires are due to the stopping effect upon reaching zero supersaturation in a catalyst droplet. This effect is specific for small droplets, which do not contain enough material at nucleation to grow a whole monolayer from liquid. Upon reaching zero supersaturation of the liquid phase, the monolayer growth rapidly continues by taking the required amount of material from the truncation, which explains the rapid increase in the truncated volume after the stopping size. In growth conditions without a stopping size, the calculated truncation volumes are much smaller and may be even unphysically small for GaAs and other III-V nanowires. The model is applied to self-catalyzed zinc blende GaAs nanowires and Au-catalyzed Si nanowires and compared to the available experimental data.

OPERA Work Group

II- Applications- and Industry-oriented material developments (WG2&3)

Sub-Bandgap Photoconductive High Voltage Switch of Mn:GaN Semiconductor



Reference: IEEE TRANSACTIONS ON ELECTRON DEVICES,

VOL. 71, NO. 9, SEPTEMBER 2024,

https://doi.org/10.1109/TED.2024.3427098.

Authors: P. Ščajev, L. Subacius, P. Prystawko and I.

Kašalynas

Laboratories: UNIPRESS(PL), FTMC(LT), VU(LT).

Techniques: MOCVD, ammonothermal method, PL, PC.

Materials: GaN semiconductors and devices

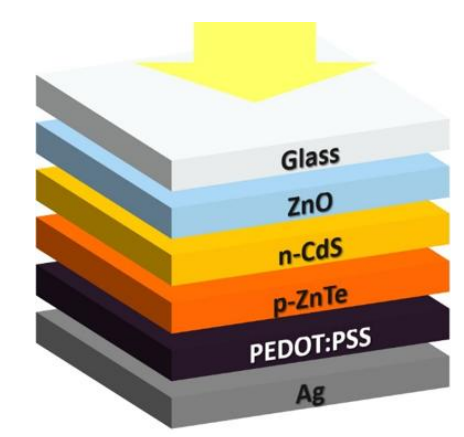
Abstract

We demonstrate the high voltage switch based on a Mn-doped GaN semiconductor involving sub bandgap photo-excitation by means of Nd:YAG laser emitting in the second harmonic. Induced bandtails of Mn were found to be photoconductive starting from the 700 nm wavelength threshold. Turn-on time of the high voltage switch was probed with short 10 ps duration laser pulses revealing the voltage pulse duration and rise time values can be as short as 1 ns and 100 ps, respectively. Relaxation of the switch photoconductivity exhibited a 2 ns decay time at low-intensity laser pulses, while at the highest intensities, it increased up to 14 ns value due to the saturation of the intermediate band or nonradiative defects. The resistance of on state was regulated up to ten orders of magnitude under the change of the laser pulse intensity, which allowed the switch to wire kilovolt voltage pulses on the load of 50 impedance. The developed high-voltage switch with performance in nanosecond time scale is beneficial for applications where high repetition rate operation is required.

OPERA Work Group

WG1 and WG2

DC current-voltage and impedance spectroscopy characterization of nCdS/pZnTe HJ



Reference: Sci Rep 14, 16115 (2024); doi:

10.1038/s41598-024-66982-2

Authors: I. Lungu, R.E. Patru, A.C. Galca, L. Pintilie, T.

Potlog

Laboratories: OIMO(MD), CHMM(RO).

Techniques: css

Materials: ZnTe, CdS, ZnO

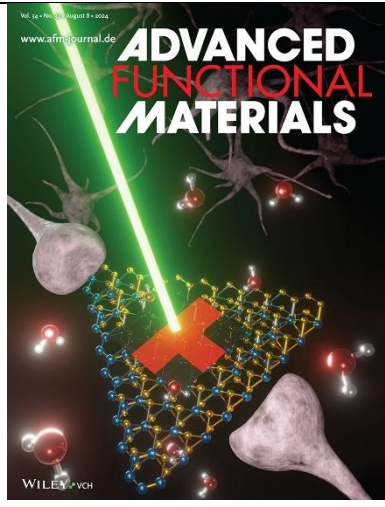
Abstract

This paper describes the electrical and dielectric behavior of the HJ by current-voltage, capacitance-voltage characteristics, and impedance spectroscopy in a temperature interval 220–350 K. A microcrystalline p-ZnTe layer and n-CdS were grown on glass/ZnO substrate by closed space sublimation method. As frontal contact to CdS, the transparent ZnO and as a back contact to ZnTe, silver conductive paste (Ag) treated at 50 °C in vacuum were used. The current–voltage results of nCdS/pZnTe HJ shows a rectifying behavior. The junction ideality factor, barrier height, and series resistance values were extracted from the rectifying curves at different temperatures. The built-in voltage, carrier concentration and depletion width were obtained from the capacitance voltage measurements. Analysis of the J-V-T and C-V-T characteristics shows that the thermionic emission and recombination current flow mechanisms dominate in the nCdS/pZnTe HJ. The dielectric study reveals that the experimental values of the AC conductivity, dielectric constant, dielectric loss, the imaginary part of the electric modulus are found to be very sensitive to frequency and temperature. The dielectric constant and dielectric loss are observed to be high at the low frequency region. The increase in the values of electric modulus with the frequency implies an increase in the interfacial polarization at the interface of nCdS/pZnTe HJ. Jonscher's universal power law shows that with increasing frequency, AC conductivity increased. The results conductivity show that the ionic conductivity and interfacial polarization are the main parameters affecting the dielectric properties of the device when the temperature changes.

OPERA Work Group

WG1 & WG2

Synaptic Plasticity and Visual Memory in a Neuromorphic 2D Memitter Based on WS₂ Monolayers



Reference: Adv. Funct. Mater. 2024, 34, 2403158 (2024);

DOI: 10.1002/adfm.202403158

Authors: F. Ferrarese Lupi, G. Milano, A. Angelini, M. Rosero-Realpe, B. Torre, E. Kozma, C. Martella, C. Grazianetti Laboratories: INRiM(It), Politecnico di Torino (It), CNR-

IMM (It), CNR-SCITEC (It).

Techniques: CVD, Raman Spectroscopy, PL.

Materials: ws₂

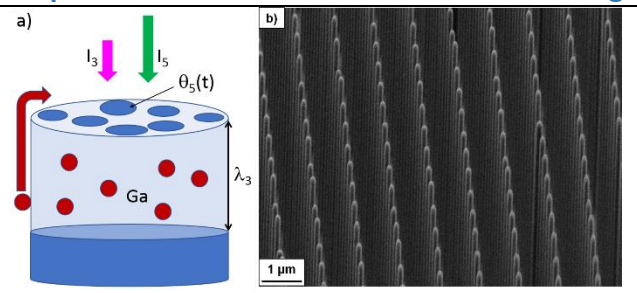
Abstract

Neuromorphic computing aims to leverage physical phenomena of adaptive materials for emulating information processing capabilities and effectiveness of biological neuronal circuits. In this framework, memristors (resistors with memory) based on 2D materials are demonstrated for the hardware implementation of highly integrated artificial neural networks. All the works reported thus far exploited electrical properties of 2D materials to emulate neuromorphic functionalities. Here, a 2D memitter (emitter with memory) is reported on that exploits the stimuli-responsive photoluminescence of a monolayer WS₂ for neuromorphic-type of data processing. A combined experimental and modeling approach reveals photoluminescent dynamics triggered by optical stimulation emulates Short-Term synaptic Plasticity and Visual Short-Term Memory typical of biological systems. While spatio-temporal processing capabilities of input signals can be used for information processing in the context of reservoir computing, the capability of the 2D memitter of sensing, processing, and memorizing-forgetting optical inputs in the same physical substrate can be utilized for in-sensor computing.

OPERA Work Group

WG1 & WG2

Importance of As and Ga Balance in Achieving Long GaAs Nanowires by Selective Area Epitaxy



Reference: Cryst. Growth Des. 2023, 23, 6, 4401–4409;

DOI: https://doi.org/10.1021/acs.cgd.3c00172

Authors: E.Chereau, V. G. Dubrovskii, G. Grégoire, G. Avit, P.Staudinger, H.Schmid, C.Bougerol, P.M. Coulon, P.A. Shields,

A.Trassoudaine, E.Gil, R.R. LaPierre, Y.André.

Laboratories: Institut Pascal (Fr), Saint Petersburg (Russia), IBM Europe (Switzerland), Institut Néel (Fr), Bath

(UK), McMaster (Canada)

Techniques: HVPE, SEM, HRTEM Materials: GaAs/GaAs(111)B

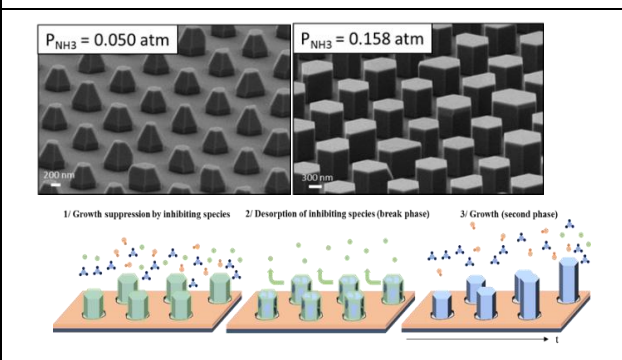
Abstract

We report on the selective area growth (SAG) of GaAs nanowires (NWs) by the catalyst-free vapor-solid mechanism. Well-ordered GaAs NWs were grown on GaAs(111)B substrates patterned with a dielectric mask using hydride vapor phase epitaxy (HVPE). GaAs NWs were grown along the (111)B direction with perfect hexagonal shape when the hole's opening diameter in SiN_x or SiO_x mask was varied from 80 to 340 nm. The impact of growth conditions and the hole size on the NW lengths and growth rates was investigated. A saturation of the NW lengths was observed at high partial pressures of As4, explained by the presence of As trimers on the (111)B surface at the NW top surface. By decreasing As4 partial pressure and decreasing the hole size, high aspect ratio NWs were obtained. The longest and thinnest NWs grew faster than a two-dimensional layer under the same conditions, which strongly suggests that surface diffusion of Ga adatoms from the NW sidewalls to their top contributes to the resulting axial growth rate. These findings were supported by a dedicated model. The study highlights the capability of the HVPE process to grow high aspect ratio GaAs NW arrays with high selectivity.

OPERA Work Group

WG1 & WG2

Circumventing the ammonia-related growth suppression for obtaining regular GaN nanowires by HVPE



Reference: Nanotechnology. 2024, 35 265604

DOI: 10.1088/1361-6528/ad3741

Authors: E. Semlali, G. Avit, Y. André, E. Gil, A. Moskalenko, P. Shields, V. G. Dubrovskii, A. Cattoni, JC. Harmand, A. Trassoudaine,

Laboratories: Institut Pascal (Fr), C2N Paris-Saclay (Fr),

Bath (UK), Saint Petersburg (Russia).

Techniques: HVPE, SE, process patterning of substrates.

Materials: GaN

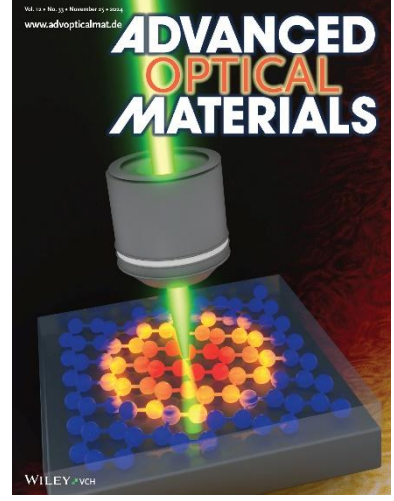
Abstract

Selective area growth by hydride vapor phase epitaxy of GaN nanostructures with different shapes was investigated versus the deposition conditions including temperature and ammonia flux. Growth experiments were carried out on templates of GaN on sapphire masked with SiN_x. We discuss two occurrences related to axial and radial growth of GaN nanowires. A growth suppression phenomenon was observed under certain conditions, which was circumvented by applying the cyclic growth mode. A theoretical model involving inhibiting species was developed to understand the growth suppression phenomenon on the masked substrates. Various morphologies of GaN nanocrystals were obtained by controlling the competition between the growth and blocking mechanisms as a function of the temperature and vapor phase composition. The optimal growth conditions were revealed for obtaining regular arrays of ~5 mm long GaN nanowires.

OPERA Work Group

WG1 & WG2

Effective Out-Of-Plane Thermal Conductivity of Silicene by Optothermal Raman Spectroscopy



Reference: Adv. Optical Mater. 12, 2401466 (2024); DOI:

10.1002/adom.202401466

Authors: E. Bonaventura, D. S. Dhungana, C. Massetti, J. Pedrini, C. Grazianetti, C. Martella, F. Pezzoli, A. Molle, E. Bonera

Laboratories: Università degli Studi di Milano-Bicocca (It), CNR-IMM (It).

Techniques: MBE, Raman Spectroscopy.

Materials: Silicene

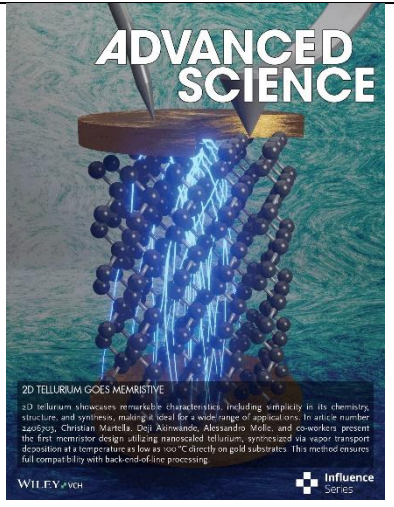
Abstract

Silicene has recently been revisited as a 2D material with potential thermoelectric applications. Here, the thermal properties of supported silicene are determined by optothermal Raman spectroscopy. Single and multilayer silicene is grown either directly on silver (Ag) substrates or on an intermediate tin (Sn) monolayer, introduced to reduce the influence of the substrate on the physical properties of silicene. Experimental values of an effective cross-plane thermal conductivity of 0.5 W/mK are obtained for silicene on Ag and 0.3 W/mK for silicene on stanene-Ag. The values of the interfacial thermal conductance, on the other hand, are 0.3 and 0.5 GW/m²K, respectively. Heterostack engineering is confirmed as a versatile strategy for extracting relevant physical parameters in silicene and for modulating the thermal response in the 2D limit.

OPERA Work Group

WG1 & WG2

Non-Volatile Resistive Switching in Nanoscaled Elemental Tellurium by Vapor Transport **Deposition on Gold**



Reference: Adv. Sci. 12, 2406703 (2025); DOI:

10.1002/advs.202406703

Authors: S. Ghomi, C. Martella, Y. Lee, P. H.-P. Chang, P. Targa, A. Serafini, D. Codegoni, C. Massetti, S. Gharedaghi, A. Lamperti, C. Grazianetti, D. Akinwande, A. Molle

Laboratories: CNR-IMM (It), Politecnico di Milano (It),

University of Texas (USA).

Techniques: VTD, Raman Spectroscopy, AFM, TEM, EELS, EDX, electrical measurements.

Materials: Tellurium

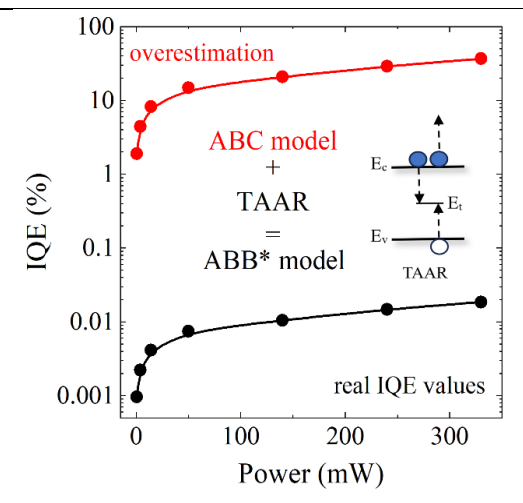
Abstract

Two-dimensional (2D) materials are promising for resistive switching in neuromorphic and in-memory computing, as their atomic thickness substantially improve the energetic budget of the device and circuits. However, many 2D resistive switching materials struggle with complex growth methods or limited scalability. 2D tellurium exhibits striking characteristics such as simplicity in chemistry, structure, and synthesis making it suitable for various applications. This study reports the first memristor design based on nanoscaled tellurium synthesized by vapor transport deposition (VTD) at a temperature as low as 100 °C fully compatible with back-end-of-line processing. The resistive switching behavior of tellurium nanosheets is studied by conductive atomic force microscopy, providing valuable insights into its memristive functionality, supported by microscale device measurements. Selecting gold as the substrate material enhances the memristive behavior of nanoscaled tellurium in terms of reduced values of set voltage and energy consumption. In addition, formation of conductive paths leading to resistive switching behavior on the gold substrate is driven by goldtellurium interface reconfiguration during the VTD process as revealed by energy electron loss spectroscopy analysis. These findings reveal the potential of nanoscaled tellurium as a versatile and scalable material for neuromorphic computing and underscore the influential role of gold electrodes in enhancing its memristive performance.

OPERA Work Group

WG1 & WG2

Internal quantum efficiency of GaAsBi MQW structure for the active region of **VECSELs**



Reference: Appl. Phys. Lett. 125, 221102 (2024).

DOI: 10.1063/5.0234853

Authors: A. Štaupienė, A. Zelioli, A. Špokas, A. Vaitkevičius, B. Čechavičius, S. Stanionytė, S. Raišys,

R.Butkutė, and E.Dudutienė

Laboratories: FTMC (OD), VU (FNI) Techniques: MBE, TDPL, ABB* method

Materials: Nb:STO/SrTiO_{3-δ}

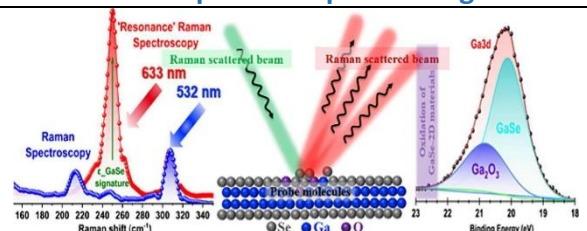
Abstract

In this work, we present a detailed study on the optical properties of GaAsBi/GaAs multiple quantum well (MQW) structure, optimized for the active area for vertical-external-cavity surfaceemitting lasers (VECSELs). The quantum structure was grown by molecular beam epitaxy with every other barrier made thinner to have a homogeneous structure with high photoluminescence (PL) intensity. PL measurements were carried out in a wide temperature range from 4 to 300 K. The PL band of 1.085 eV was attributed to the optical transition in GaAsBi/GaAs QWs with 8.0%Bi. The S-shaped temperature dependence of PL peak positions showed high localization effect of 30 meV. The internal quantum efficiency (IQE) was evaluated for the bismide structures with a modified ABB* method, which includes contribution from trap-assisted Auger recombination. The calculations showed low IQE of value less than 0.025% for GaAs0.92Bi0.08/GaAs 12 QWs structure, which was explained by the low growth temperature, resulting in a high density of point defects in the material.

OPERA Work Group

WG1. WG2

Spectroscopic investigation of oxidation in GaSe 2D layered materials



Reference: Microelectron. Eng. 2024, 294, 112256

DOI: 10.1016/j.mee.2024.112256

Authors: B. Smiri, R. Bernardin, M. Martin, H. Roussel, J.L. Deschanvres, E. Nolot, N. Rochat, F. Bassani, T. Baron,

and B. Pelissier

Laboratories: LTM(Fr), LETI(Fr).
Techniques: MOCVD, Raman, PL, XPS

Materials: 2D-GaSe

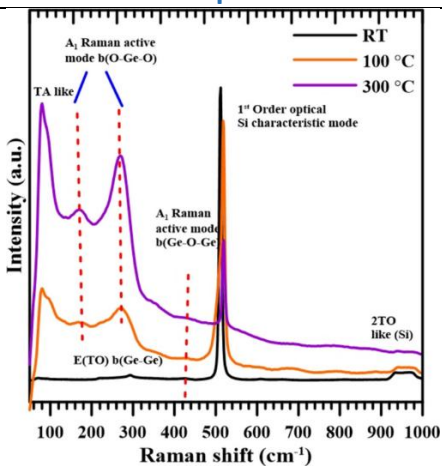
Abstract

GaSe, a two-dimensional layered metal monochalcogenide, has recently attracted growing interest due to its unique electronic properties and potential technological applications. In this study, we investigate the oxidation mechanisms and properties of GaSe exposed to air for different durations, with the intensive use of Raman spectroscopy, combined with atomic force microscopy (AFM), photoluminescence (PL), and X-ray photoelectron spectroscopy (XPS). Raman analysis reveals the oxidation of GaSe, resulting in the formation of a thin layer comprising Ga₂Se₃, Ga₂O₃, and amorphous selenium. Utilizing these signatures, oxidation is then tracked. Raman spectroscopy reveals that GaSe layer becomes oxidized almost immediately after exposure to air. However, the oxidation is a selflimiting process, taking roughly 15 min to construct an 8 Å thick layer of Ga₂O₃. XPS analysis shows a good agreement with Raman analysis. The polarized Raman study suggests that the Ga₂Se₃ and Ga₂O₃ layers tend to reach an oriented structural state over time. In ambient conditions, the intensity of all Raman modes and the luminescence decreases, linked to reduction in GaSe thickness. By using various Raman excitation wavelengths, we highlight the depth-dependent oxidation dynamics in this 2D layered GaSe material.

OPERA Work Group

WG1 & WG2

Effect of substrate temperature on Raman study and optical properties of GeOx/Si thin films



Reference: Journal of the Australian Ceramic Society (2024) 60:591–599. https://doi.org/10.1007/s41779-023-00961-0
Authors: D Baghdedi, H Hopoğlu, İ Demir, İ Altuntaş, N

Abdelmoula, EŞ Tüzemen

Laboratories: Sivas Cumhuriyet University Nanophotonics Application and Research Center -CUNAM (Tr), and Laboratory of Multifunctional Materials and Applications (LaMMA)-University of Sfax (Tn)

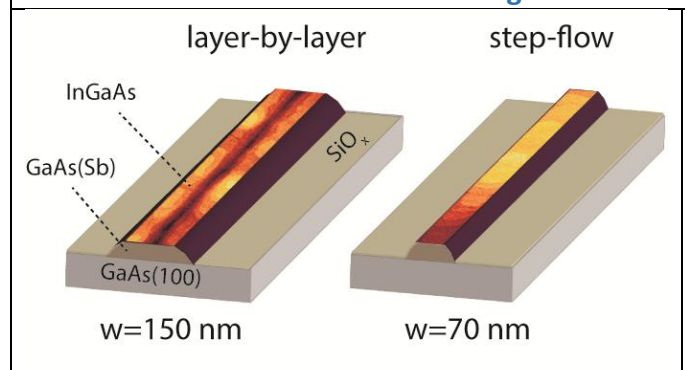
Techniques: RF Magnetron Sputtering, XRD, Raman

Materials: GeOx, Si

In this study, GeOx thin films were deposited onto Si substrates using the RF magnetron sputtering method. We looked at how the temperature of the substrate affected the Raman spectra and optical characteristics of GeOx thin films. X-ray diffraction was utilized to examine the crystal structure, and a scanning electron microscope was utilized to measure the thickness. In order to investigate the local structure and bonding characteristics, Raman spectroscopy was used. The refractive index, extinction coefficient, and dielectric parameters were calculated using spectroscopic ellipsometry for the 300-1100 nm spectral region. Refractive index and extinction coefficient spectral patterns were discovered by using a sample-air optical model to analyze the experimental ellipsometric data. Notably, a considerable rise in the refractive index was accompanied by a rise in substrate temperature.

OPERA Work Group

Scale-dependent growth modes of selective area grown III-V nanowires



Reference: Nano Lett. 2024, 24, 45, 14198–14205; DOI: https://doi.org/10.1021/acs.nanolett.4c03283

Authors: D. V. Beznasyuk, S. Marti-Sanchez, G. Nagda, D. J.

Carrad, J. Arbiol, T. Sand Jespersen

Laboratories: DTU Energy (dk), ICN2 (sp), ICREA (sp)

Techniques: MBE, selective area growth, AFM, HR STEM, SEM

Materials: GaAs(100), GaAs(Sb), InGaAs

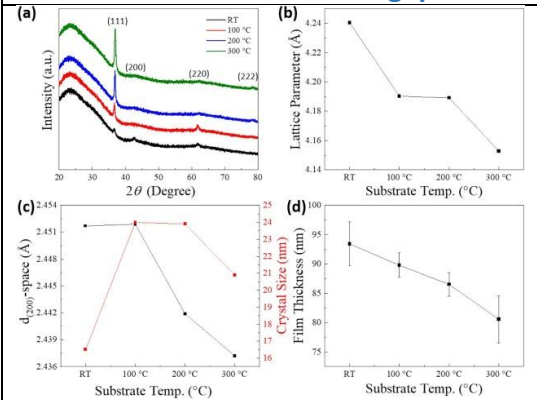
Abstract

Due to their flexible geometry, in-plane selective area grown (SAG) nanowires (NWs) encompass the advantages of vapor–liquid–solid NWs and planar structures. The complex interplay of growth kinetics and NW dimensions provides new pathways for crystal engineering; however, their growth mechanisms remain poorly understood. We analyze the growth mechanisms of GaAs(Sb) and InGaAs/GaAs(Sb) inplane SAG NWs using molecular beam epitaxy (MBE). While GaAs(Sb) NWs consistently follow a layer-by-layer growth, the InGaAs/GaAs(Sb) growth transitions from step-flow to layer-by-layer and layer-plus-island depending on the InGaAs thickness and the NW dimensions. We extract the diffusion lengths of Ga adatoms along the [1-10] and [110] directions under As₂ during GaAs(Sb) growth. Our results indicate that Sb may inhibit the layer-by-layer to step-flow transition. Our findings show that different growth modes can be achieved in the MBE of in-plane SAG NWs grown on the same substrate and highlight the importance of the interplay with NW dimensions.

OPERA Work Group

WG1 & WG2

Optical properties of NiO films: Effect of nitrogen-doping, substrate temperature and band gap estimation using machine learning



Reference: Materials Science & Engineering B 307 (2024) 117507

https://doi.org/10.1016/j.mseb.2024.117507

Authors: Kaya, D., Hopoğlu, H., Çelik, A., Akyol,
M., Karadag, F., Tüzemen, E. Ş., & Ekicibil, A.

Laboratories: Sivas Cumhuriyet University
Nanophotonics Application and Research Center CUNAM (Tr), Department of Advance Materials and
Nanotechnology at Cukurova University (Tr),
Department of Materials Science and Engineering,
and Faculty of Engineering at Adana Alparslan
Turkes Science and Technology University (Tr)

Techniques: Sputtering, XRD, SEM-EDX, UV-Vis-NIR spectrophotometer

Materials: NiO

In this study, nickel oxide (NiO) thin films were synthesized on glass substrates using RF magnetron sputtering with varying nitrogen (N) doping ratio and substrate temperatures to explore modifications in their structural, morphological, and optical properties. The films were prepared using a high-purity NiO target under controlled sputtering conditions. Structural analysis by X-ray diffraction revealed an improvement in crystallinity in the (2 0 0) direction with increasing N ratio. In contrast, higher N ratio led to the suppression of (1 1 1) and (2 2 0) peaks, indicating a significant influence of N on the crystal structure and orientation. The films' thickness and morphology, examined using scanning electron microscopy and energy-dispersive X-ray spectroscopy, showed uniform and homogeneous growth with smooth surface topologies. Optical properties, assessed by UV-Vis-NIR spectrophotometry, demonstrated a decrease in transmittance and a redshift in the absorption edge with increased N doping, corresponding to a narrowing of the energy bandgap from 3.7 eV to 3.45 eV. This bandgap reduction is attributed to N incorporation substituting oxygen sites, introducing defect states within the band structure. Additionally, the impact of substrate temperature on film growth enhanced crystallinity and orientation along the (1 1 1) plane at higher temperatures, with a simultaneous reduction in film thickness due to increased adatom mobility and potential thermal decomposition. The evaluation of Kernel Ridge Regression (KRR) and Ridge Regression (RR) models revealed their effectiveness in predicting band gap values for thin films at varying substrate temperatures and thicknesses. While RR excelled in predicting a band gap of 3.6 eV for a film with a substrate temperature of 24 °C and a thickness of 112.7 nm, KRR outperformed in predicting a band gap of 3.65 eV for a film with a substrate temperature of 24 °C and a thickness of 107 nm. These findings elucidate the dual influence of N doping and substrate temperature on enhancing the functional properties of NiO thin films, promising for applications in optoelectronic devices and gas sensors.

OPERA Work Group

A Study on the Growth Conditions Role in Defining InGaAs Epitaxial Layer Quality

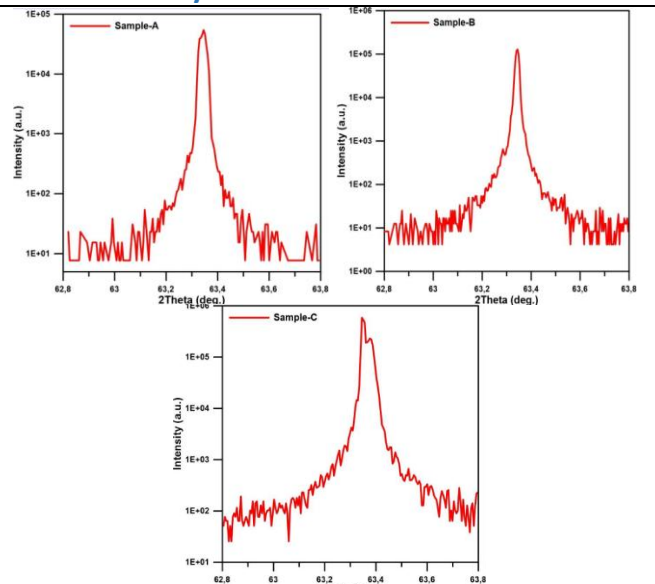


Fig. HRXRD measurement of sample A, B, and C Reference: Cumhuriyet Sci. J., 45(2) (2024) 400-406

https://doi.org/10.17776/csj.1441702 Authors: Demir, M., & Elagöz, S.

Laboratories: Sivas Cumhuriyet University Nanophotonics

Application and Research Center - CUNAM (Tr)

Techniques: MOVPE, XRD, Hall effect spectrophotometer

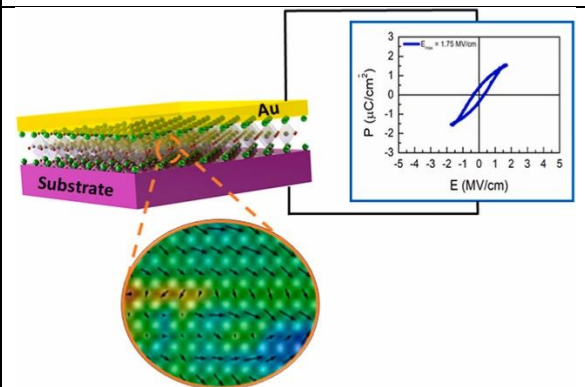
Materials: In_xGa_{1-x}As

This study delves into the epitaxial growth and characterization of In_xGa_{1-x}As layers on InP substrate, a critical area in the development of high-performance III-V semiconductor devices. $In_xGa_{1-x}As$ is renowned for its superior electron mobility and broad spectral response, making it indispensable in applications ranging from photodetectors to quantum cascade lasers. Employing a horizontal flow reactor MOVPE (metal-organic vapor phase epitaxy) technique, we meticulously grew n- In_xGa_{1-x}As epilayers under varying conditions to investigate the impact of indium content, growth temperature, and V/III ratio on the material's structural, optical, and electrical properties. HRXRD (Highresolution X-ray diffraction) and Hall-effect measurements provided insights into the correlation between growth parameters and epitaxial layer quality, including dislocation density and carrier mobility. Our findings highlight the delicate balance required in the growth process to optimize the In_xGa_{1-x}As/InP structure's performance for advanced semiconductor applications. The research underscores the potential of tailored In_xGa_{1-x}As layers to push the boundaries of current photonics and optoelectronics technologies, emphasizing the importance of growth condition optimization for enhancing device efficiency and thermal stability.

OPERA Work Group

WG2

Ferroelectric behavior arising from polar topologies in epitaxially strained SrTiO_{3-δ} ultrathin films



Reference: Materials Nano Today. 26 (2024) 100486.

DOI: 10.1016/j.mtnano.2024.100486

Authors: T. Rodrigues, J. P.B. Silva, F. Figueiras, M.R. Soares, R. Vilarinho, J. A. Moreira, I. Çaha, F. L. Deepak, B. Almeida Laboratories: CF-UM-UP (PT), LapMET (PT), IFIMUP (PT),

CICECO (PT), INL (PT)

Techniques: IBSD, STEM/EDS, HRXRD, Raman Spectroscopy, SEM, PFM, (P-E) hysteresis loop measurement

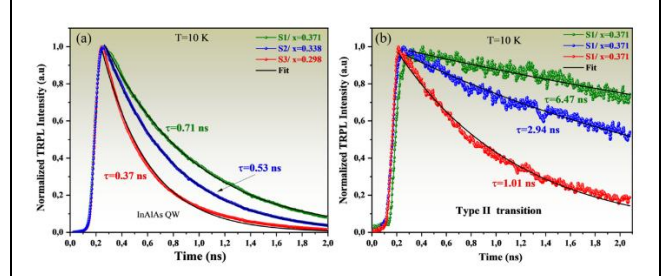
Materials: Nb:STO/SrTiO_{3-δ}

Abstract

In this work, we show that epitaxially strained $SrTiO_{3-\delta}$ thin films, grown by ion-beam sputtering onto (001)Nb:SrTiO₃ substrates, exhibit a ferroelectric behavior. At the atomic-scale, through high-angle annular dark-field scanning transmission electron microscopy (HAADF-STEM) images, it was possible to identify the presence of polar nanoregions with non-trivial polar topological structures in the $SrTiO_{3-\delta}$ film, which are induced through oxygen vacancies. To further confirm the presence of strained regions with a polar structure, Raman spectroscopy and high-resolution X-ray diffraction were employed and it was possible to confirm the presence of a tetragonal structure in the SrTiO_{3- δ} film, with a tetragonality ratio (c/a) of 1.005. Scanning probe microscopy and macroscopic polarization-electric field hysteresis loops show ferroelectric behavior with maximum polarization of \sim 1.5 μ C/cm2, remnant polarization of \sim 0.4 μ C/cm2 and coercive field of ~0.3 MV/cm. This work opens a window for exploring novel polar topological effects in sub-10 nm thin film materials for non-volatile memory application.

OPERA Work Group

Influence of Indium Composition on InAlAs QCLs



Reference: This is a preprint; it has not been peer reviewed by a journal.

https://doi.org/10.21203/rs.3.rs-4670192/v1

Authors: S Badreddine, D Ilkay, H Abir, H Carrère, A Ismail, A Mlayah, M Hassen, M Xavier*

Laboratories: Sivas Cumhuriyet University Nanophotonics Application and Research Center -CUNAM (Tr), Université de Toulouse, INSA-CNRS-UPS, LPCNO

Techniques: MOVPE, XRD, Raman, PL, Time-resolved PL

(TRPL)

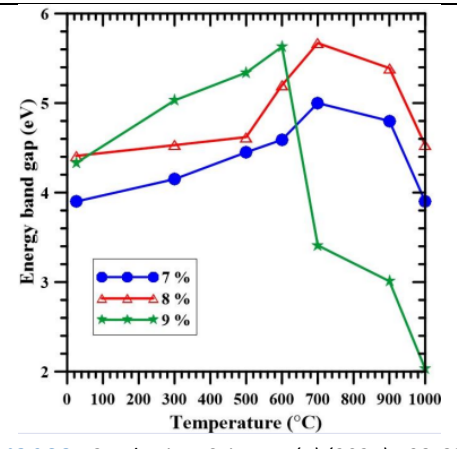
Materials: InAIAs,InP

In this work, we explored the impact of indium composition (x) on the structural and optical characteristics of InxAl1-xAs layers within the context of quantum cascade laser (QCL) structures grown on InP (100) substrates using the Metal Organic Vapor Phase Epitaxy (MOVPE) method. The quality of the InxAl1-xAs QCL is notably influenced by the growth with low indium composition, evident in terms of crystallinity, interface sharpness, and optical properties. The properties of the InAsP layer at the InP/ InxAl1-xAs junction are particularly sensitive to the indium composition. A drop below 0.52 in indium composition leads to a substantial lattice mismatch between the InxAl1-xAs layer and the InP substrate, typically exceeding [3 8]%. This mismatch induces defects or traps within the bandgap, significantly impacting carrier localization in this system. Our study demonstrates that cultivating InxAl1-xAs with a low indium concentration results in a strained (latticemismatched) InxAl1-xAs layer. This finding is significant as it can be leveraged to balance strain in high indium content InGaAs layers, particularly in the context of applications involving quantum cascade lasers.

OPERA Work Group

WG2

Production of GeOx Films at Different Oxygen Flow Rates and Different Annealing Temperatures and Examination of Energy Band Gaps using Kubelka Munk Method



Reference: Cumhuriyet Sci. J., 45(4) (2024) 598-603

https://doi.org/10.17776/csj.1482632

Authors: Özdemir, A., Kızıl, Ş. G., & Tuzemen, E. S.

Laboratories: Sivas Cumhuriyet University

 ${\it Nanophotonics\ Application\ and\ Research\ Center\ -CUNAM}$

(Tr)

Techniques: Sputtering, UV-Vis-NIR

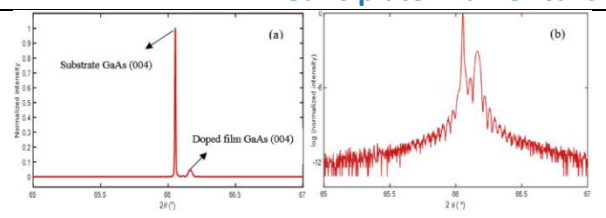
spectrophotometer

Materials: GeOx

In this study, GeOx films were grown on silicon substrates using the Radio Frequency (RF) Magnetron Sputtering method at different oxygen flow rates and annealing temperatures. The films were produced at a substrate temperature of 250°C and a working pressure of 13 mTorr. Subsequently, the films were annealed at temperatures of 300°C, 500°C, 600°C, 700°C, 900°C, and 1000°C. Total and diffuse reflection measurements were performed to investigate the optical properties of the films. Energy band gaps were determined using diffuse reflection measurements and they were calculated using the Kubelka-Munk method. It was observed that the energy band gap increased with increasing oxygen ratio. Additionally, annealing temperatures were found to cause changes in the energy band gaps.

OPERA Work Group

Real, imaginary and complex branches of Lamb waves in p-type piezoelectric semiconductor GaAs plate: Numerical and experimental investigation



Reference: Materials Science in Semiconductor

Processing 183 (2024)

https://doi.org/10.1016/j.mssp.2024.108743

Authors: Dhib, A., Njeh, A., Othmani, C., Takali, F., Salah,

I. B., Demir, I., Zhang, B., & Altinsoy, M. E.

Laboratories: Sivas Cumhuriyet University

Nanophotonics Application and Research Center -CUNAM (Tr), Laboratory of Physics of Materials at University of Sfax (Tn), Henan International Joint Laboratory of Advanced Electronic Packaging Materials Precision Forming at Henan Polytechnic University (Cn)

Techniques: XRD, Hall effect

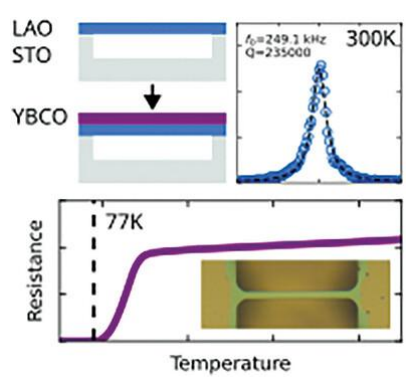
Materials: GaAs, ZnO

First, we experimentally measure the concentration of holes of the piezoelectric semiconductor (PSC) Gallium arsenide (GaAs) material based on the Hall effect measurement. We then numerically calculate the Lamb wave characteristics in a p-type PSC GaAs plate using this measured value of the concentration of holes (estimated at approximately $p_0 = 3.5431 \times 10^{25} \text{m}^{-3}$). To guarantee the coupling effect that makes the Lamb wave a piezo-active wave, the GaAs crystal is oriented in a specific orientation of (110) plane. Ordinary differential equation (ODE) method is employed to calculate the dispersion curves, 3D view of the mechanical displacements, 3D view of the electric potential and 3D view of the concentrations of holes. Results show that the appearance of the complex branches of the Lamb modes coincides with the vanishing of the imaginary part of the wavevector (Im(k1)) to zero, which is a very remarkable finding that has not been discussed in previous studies. Meanwhile, these complex branches start exactly at the point of Zero-groupvelocity (ZGV). Moreover, the present work highlights the hole drift characteristics of PSC GaAs and provides a critical comparative discussion with those published by (Zhu et al., 2018) for the PSC ZnO plate. Accordingly, the "Screening effect" phenomenon that is based on the positive holes in the negative electric potential region is discussed. The present results provide a theoretical and fundamental guidance on the development of smart devices based on the PSC GaAs material.

OPERA Work Group

WG2

Integration of High-Tc Superconductors with High-Q-Factor Oxide Mechanical Resonators



Reference: Adv. Funct. Mater. 2024, 34, 2403155;

doi; <u>10.1002/adfm.202403155</u>.

Authors: N. Manca, A. Kalaboukhov, A. E. Plaza, L. Cichetto Jr., E. Wahlberg, E. Bellingeri, F. Bisio, F. Lombardi, D. Marré, L. Pellegrino Laboratories: CNR-SPIN (it), Chalmers University of Technology (se), RISE Research Institutes of Sweden (se). Univ. of Genoa (it) Techniques: PLD, optical lithography, XRD, AFM, optomechanics

Materials: SrTiO₃, LaAlO₃, YBCO

Abstract

Micro-bridge mechanical resonators are realized from crystalline LaAlO3 transparent thin films deposited on SrTiO3 substrates. Such resonators have low surface roughness and a high mechanical Q-factor, paving the way for the realization of oxide-based resonant sensors. They are employed as templates for the growth of superconducting YBCO single crystal thin films. A superconducting resonator having mechanical Q-factor around 180k at room temperature is demonstrated.

OPERA Work Group

Characterization of SiNx grown at different nitrogen flow and prediction of refractive index using artificial neural networks

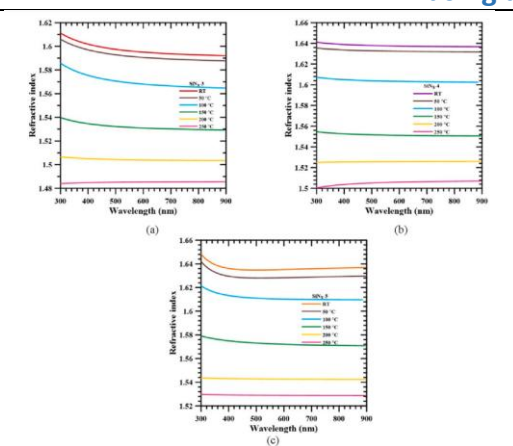


Fig. Refractive index of (a) SiNx_3 (b) SiNx_4, (c) SiNx 5

Reference: Physica B: Condensed Matter 695 (2024) 416581

https://doi.org/10.1016/j.physb.2024.416581 Authors: Yüksek, A. G., Horoz, S., Demir, İ.,

Altuntaş, İ., & Tüzemen, E. Ş.

Laboratories: Sivas Cumhuriyet University Nanophotonics Application and Research Center -CUNAM (Tr)

Techniques: Sputtering, XRD, SEM-EDX, UV-Vis-NIR spectrophotometer

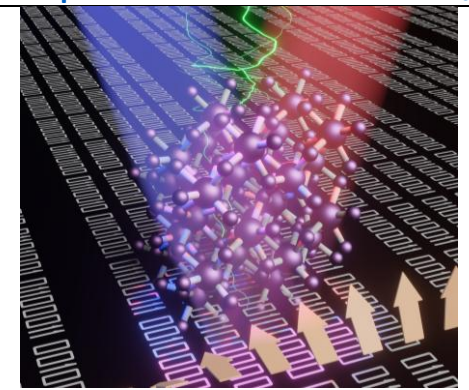
Materials: sinx

SiNx films were grown on silicon substrates by Radio Frequency (RF) magnetron sputtering deposition. The effect of nitrogen flow on the structural and optical properties of the obtained films was investigated using X-ray diffraction, Scanning Electron Microscopy (SEM), UV-Vis-NIR spectrophotometer and spectroscopic ellipsometer, respectively. XRD spectra of the films showed that all films belong to amorphous structure. SEM photographs of SiNx films were analyzed. As a result of the analysis, it was observed that the surfaces of the films had a homogeneous and smooth structure as the nitrogen flow increased. The total and diffuse reflectance spectra of the films were measured, and the energy band gaps of the films were determined using the Kubelka-Munk function by using the diffuse reflectance. It was observed that the energy band gap changed as the nitrogen percentage increased. The refractive index of all films was obtained as a function of temperature using a spectroscopic ellipsometer. In the second part of this study, we focused on predicting the temperature dependent refractive indices of the nitrogen flow-dependent films using Artificial Neural Networks (ANN). For the training of the ANN model, wavelength and temperature values from experimental data were used as input and refractive index as output parameters. The simulation and prediction results obtained from this model are compared with the experimental data and interpreted. It is concluded that the ANN approach is suitable for simulating and predicting the temperature dependent refractive index. The models successfully trained with ANN will be especially preferred for predicting the refractive indices of SiNx films, which cannot be measured experimentally, thus providing predictions in non-experimental ranges. In particular, the results obtained by focusing on the ability of the developed artificial neural network (ANN) models to predict the optical properties of SiNx films and their potential to provide information in nonexperimental conditions, offer a new approach to quickly and effectively evaluate the optical properties of SiNx films. This approach reveals the importance of artificial intelligence-based methods in materials characterization studies.

OPERA Work Group

WG2

Photovoltaic-driven dual optical writing and non-destructive voltage-less reading of polarization in ferroelectric Hf_{0.5}Zr_{0.5}O₂ for energy efficient memory devices



Reference: Nano Energy 123, 109384 (2024); doi; 10.1016/j.nanoen.2024.109384..

Authors: H. Tan, A. Quintana, N. Dix, S. Estandía, J. Sort, F.

Sánchez, I. Fina

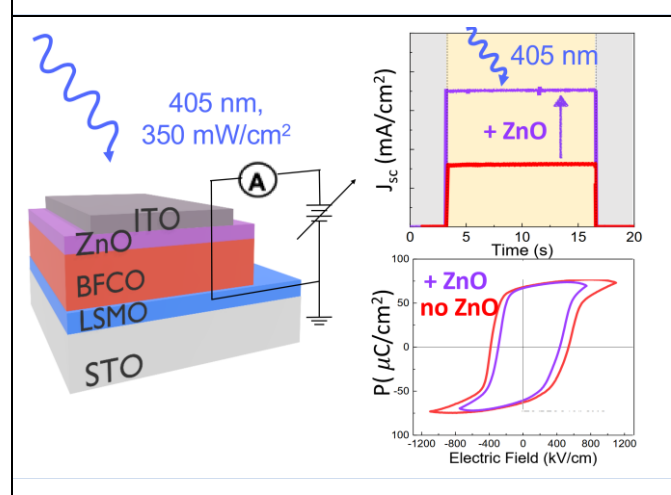
Laboratories: ICMAB, UAB. **Techniques:** PLD, electrical Materials: HfO2, ferroelectric,

Abstract

Ferroelectric doped hafnium oxide constitutes, at present, an intensively investigated candidate material to develop outperforming non-volatile memory devices. We report reading and writing of the ferroelectric polarization with light in $Hf_{0.5}Zr_{0.5}O_2/Nb:SrTiO_3$ structures, where light is absorbed at the interface between the two materials, thereby enabling both processes. Reading of ferroelectric polarization is accomplished through the induced short-circuit photocurrents, which is a pathway towards voltage-less-non-destructive reading. Optical writing allows remote and contact-less switching of ferroelectric polarization, without the need for external voltages. The presence or absence of a Pt capping layer is crucial for the aforementioned read/write operations. If top Pt is present, photocarriers flow, resulting in short-circuit photocurrent, whose magnitude is modulated by the induced depolarization field. Instead, if Pt is ...

OPERA Work Group

Interface Engineering in All-Oxide Photovoltaic Devices Based on Photoferroelectric BiFe_{0.9}Fe_{0.1}O₃ Thin Films



Reference: ACS Appl. Electron. Mater. 2024, 6, 11, 8251-8259; https://doi.org/10.1021/acsaelm.4c01533

Authors: P. Machado, P. Salles, A. Frebel, G. De Luca, E. Ros, C. Hagendorf, I. Fina, J. Puigdollers, M. Coll

Laboratories: ICMAB- CSIC (Spain), UPC (Spain), TU Darmstadt (Germany), Fraunhofer Institute (Germany)

Techniques: CSD, ALD, Sputtering, XPS, XRD, ferroelectric loops

Materials: BiFeO₃, ZnO, La_{0.7}Sr_{0.3}MnO₃, ITO

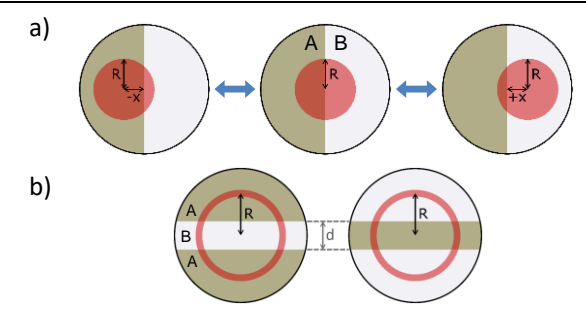
Abstract

In this work, we determine the influence of incorporating a ZnO layer on the ferroelectric and photoresponse behavior epitaxial BiFe_{0.9}Co_{0.1}O₃ (BFCO)-based heterostructure. The device is completed with Sn-doped In2O3 (ITO) and La_{0.7}Sr_{0.3}MnO₃ (LSMO) electrodes. This alloxide system is stable under ambient conditions and displays robust ferroelectricity. The coupled ferroelectricityphotoresponse measurements demonstrate that the short circuit current can be modulated by ferroelectric polarization in up to 68% under blue monochromatic light. Also, the responsivity of the system with the ZnO-modified interface is larger than that of the system with no ZnO. Complementary band energy alignment studies reveal that the observed increase in the short circuit current density of the device with ZnO is attributed to lower Fermi level energy at the ZnO/BFCO interface compared to the ITO/BFCO interface, which reduces charge recombination. Therefore, this study provides useful insights into the role of the ZnO interface layer in stable BFO-based devices to further explore their viability for potential optoelectronic applications.

OPERA Work Group

WG2

Demonstration of Two Multi-Component Target Ablation Approaches and Their Application in **Combinatorial Pulsed Laser Deposition**



Reference: Advanced Physics Research 3, 2300140 (2024); DOI: https://doi.org/10.1002/apxr.202300140

Authors: A Jörns, H von Wenckstern, S Vogt, P Schlupp, M Grundmann

Laboratories: Universität Leipzig (De) Techniques: PLD, XRD, SEM-EDX

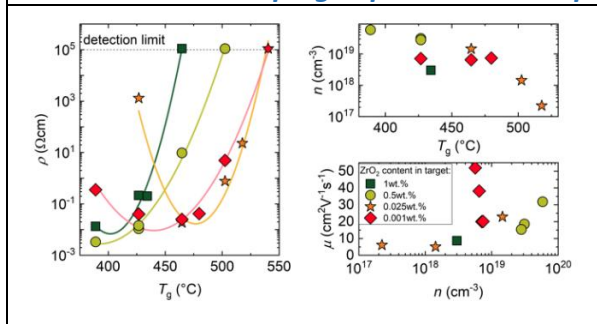
Materials: Zinc tin oxide

Abstract

Combinatorial materials synthesis significantly accelerates the discovery and characterization of novel functional solids. In recent years, various methods for realizing lateral or compositional gradients in the growth direction have been developed at Leipzig University. Here, we present variants of combinatorial Pulsed Laser Deposition that uses multi-segment targets for ablation. Using a target composed of two semicircular segments A and B, the time-averaged composition of the material flux is controlled by shifting the target's axis of rotation by x, as shown in figure a). A stoichiometric composition AB is obtained for x=0, while A-rich (B-rich) composition is obtained for negative (positive) x values. Another approach uses a segmentations ABA or BAB as shown in figure b). Here the composition of a thin film is determined by the radius R of the ablation track. For an ABA segmentation, small (large) ablation track radii R results in B-rich (A-rich) thin film compositions. Thus, both approaches allow the creation of discrete composition material libraries from a single target and also enable to realize compositional gradients in growth direction. In the manuscript, the methodology is introduced in detail and physical properties of zinc-tin-oxide thin films grown by the two novel approaches are compared to layers with similar composition obtained from a conventional PLD process.

OPERA Work Group

Zr-doping in pulsed-laser-deposited α-Ga₂O₃ for device applications



Reference: Physical Review Applied **21**, 064016 (2024); DOI: https://doi.org/10.1103/PhysRevApplied.21.064016

Authors: S. Vogt, C. Petersen, H. von Wenckstern, M.

Grundmann, T. Schultz, N. Koch

Laboratories: Universität Leipzig (De)

Techniques: PLD, XRD, van der Pauw, Current-Voltage

Characteristics

Materials: Ga₂O₃

Abstract

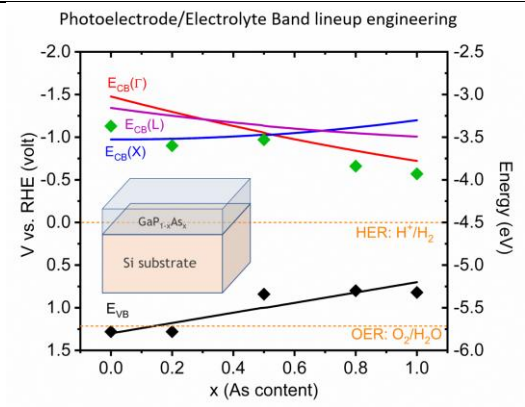
Ga₂O₃ is a highly promising material for high-power electronics and solar blind photo-detectors due to its wide bandgap. It crystallizes in different polymorphs, of which the monoclinic β-polymorph is thermodynamically stable, but the rhombohedral lpha-phase has the highest bandgap of about 5.3eV and thus the highest expected electric breakdown field. α -Ga $_2$ O $_3$ can be grown on isostructural α -Al₂O₃ substrates, however, the growth of conductive, device-ready thin films remains challenging. We fabricated electrically conductive $\alpha\text{-}Ga_2O_3$:Zr thin films by pulsed laser deposition on an undoped α -Ga₂O₃ buffer layer on m-plane α -Al₂O₃ substrates. The free carrier concentration n can be systematically varied from 10^{17} cm⁻³ to 6×10^{19} cm⁻³ via the ZrO₂-content in the PLD target and the growth temperature as shown in the figure. In general, an increasing growth temperature results in a decreasing n and an increasing carrier mobility resulting in an initial decrease of resistivity for lower growth temperature until a minimum is reached. A further increase in growth temperature increases the resistivity due to the decrease of n.

For demonstrator devices thin films with low and intermediate n were processed to Schottky barrier diodes that showed exceptional current rectification of eight orders of magnitude and higher. These results stimulate further research on α -Ga₂O₃ and its implementation in high-power devices.

OPERA Work Group

WG2

Photoelectrode/electrolyte interfacial band lineup engineering with alloyed III–V thin films grown on Si substrates



Reference: J. Mater. Chem. C, 2024,12, 1091-1097;

DOI: https://doi.org/10.1039/D3TC02556J

Authors: M. Piriyev, G. Loget, Y. Léger, H. V. Le, L. Chen, A. Létoublon, T. Rohel, C. Levallois, J. Le Pouliquen, B. Fabre, N. Bertru and C. Cornet.

Laboratories: Institut FOTON (Fr), ISCR (Fr), Tianjin Key Laboratory (Cn).

Techniques: MBE, SEM, XRD, AFM, Ellipsometry, PEC J-V, Mott-Schottky

violi-scriotiky

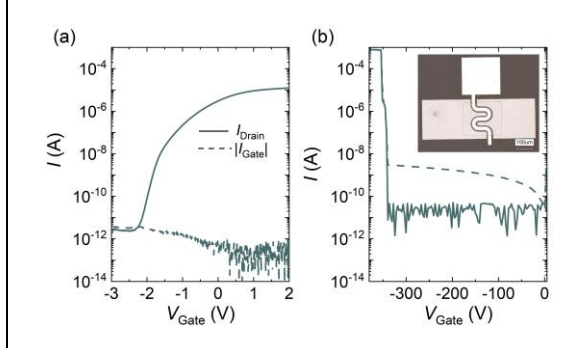
Materials: GaPAs/Si(001)

Abstract

In this work, we demonstrate how the classical concept of band gap engineering usually used in III-V semiconductor devices can be extended to the engineering of the band lineup between semiconducting photoelectrodes and electrolytes. performances of photoelectrodes made of GaP1-xAsx epilayers in the full compositional range and grown on low-cost Si substrates were studied and compared with those of photoelectrodes grown on GaAs and GaP substrates. We first show that the changes of incident photon to current conversion efficiency (IPCE) with the As content in GaP1-xAsx alloys are related to the band gap nature (direct or indirect) and band gap energy variations. Then, from flat band potential measurements during Mott–Schottky experiments, valence and conduction band energies of GaP1-xAsx alloys are positioned versus the reversible hydrogen potential. A weak change of conduction band energies and a large evolution of valence band energies are obtained, in good agreement with expected theoretical trends. Such results show that both band gaps and semiconductor/electrolyte band lineups can be engineered through alloying of III-V semiconductors deposited on silicon substrates. This band lineup engineering strategy is expected to be of great interest to address specific redox reactions in the electrolyte, provided that suitable protecting or passivating layers can be used to limit surface/interface recombination.

OPERA Work Group

Lateral a-Ga O₃:Zr metal—semiconductor field effect transistors



Reference: Appl. Phys. Lett 125, 253507 (2024); DOI:

https://doi: 10.1063/5.0220211

Authors: S. Vogt, D. Splith, S. Köpp. P. Schlupp. C. Petersen, H. von Wenckstern and M. Grundmann

Laboratories: Universität Leipzig (De)

Techniques: PLD, XRD, Magnetron Sputtering, Current-Voltage, Output and Transfer Characteristics

Materials: Ga₂O₃

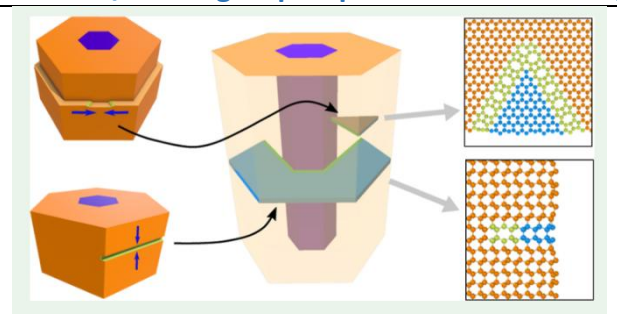
Abstract

Ga₂O₃ is a material that shows great promise for use in high-power electronics and solar blind photo-detectors because of its wide bandgap. It crystallizes in different polymorphs, of which the monoclinic β-polymorph is thermodynamically stable. However, the rhombohedral α -phase has the highest bandgap of about 5.3eV and thus the highest expected electric breakdown field. Electrically conductive, 30nm thick α-Ga₂O₃:Zr thin films were grown by pulsed laser deposition (PLD) on a α -Ga₂O₃ buffer layer on m-plane α -Al₂O₃ substrates. Two distinct layouts of metal-semiconductor field effect transistors were realized and the output, transfer and breakdown characteristics were thoroughly investigated. In figures a) and b), the transfer characteristics for one of the layouts are shown as an example. The most advanced devices demonstrated to date exhibit a current on/off ratio of over nine orders of magnitude, a sub-threshold swing of less than 200mV/dec, and an electrical breakdown field of more than 1.3MV/cm. These findings establish the current state-ofthe-art for of α -Ga₂O₃-based high-power MESFETs.

OPERA Work Group

WG2

2H-Si/Ge for group-IV photonics: on the origin of extended defects in core-shell nanowires



Reference: ACS Applied Nano Materials 7, 9396-9402 (2024) doi 10.1021/acsanm.4c00835

Authors: F. Rovaris, W. H. J. Peeters, A. Marzegalli, F. Glas, L. Vincent, L. Miglio, E. P. A. M. Bakkers, M. A. Verheijen, E. Scalise Laboratories: Univ. Milano-Bicocca (Dept. Mater. Sci.), TU Eindhoven, C2N

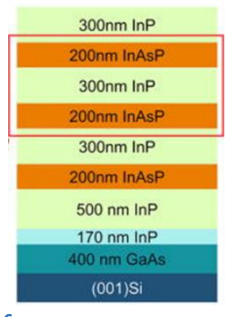
Techniques: MOVPE, TEM, modeling, machine learning Materials: Nanowires of elemental semiconductors

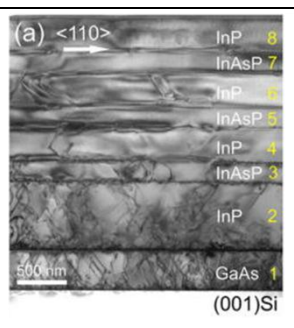
Abstract

The nucleation mechanism of ubiquitous basal stacking faults observed in hexagonal Si/Ge nanowires is still an enigma. These defects may hinder the exploitation of hexagonal Si/Ge for nano-optoelectronics and quantum technologies. In this work, the formation of the I3 basal stacking faults is investigated at the atomistic level, and results are compared to the experimental findings. We propose that these extended defects are caused by dislocation lines elongated in (11-20) directions, which in turn arise from glide terminations of the step edges when two growing fronts run into each other.

OPERA Work Group WG1, WG2

Effective InAsP dislocation filtering layers for InP heteroepitaxy on CMOS-standard (001) silicon





Reference: Appl. Phys. Lett. 125(8), 082102 (2024);

DOI: 10.1063/5.0219507

Authors: S. Liu, B.-P. Ratiu, H. Jia, Z. Yan, K.M. Wong, M.

Martin, M. Tang, T. Baron, H. Liu, and Q. Li,

Laboratories: Cardiff University(UK), LTM (Fr), UCL (UK)

Techniques: MBE, MOCVD, ECCI, TEM, XRD

Materials: InP/Si(001)

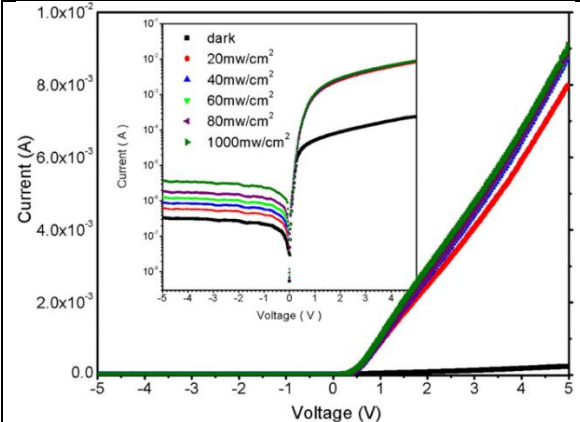
Abstract

In this work, we report InAsP-based dislocation filter layers (DFLs) for InP heteroepitaxy on CMOS-standard (001) Si substrates, demonstrating a threading dislocation density of $3.7 \times 10^7 \text{ cm}^{-2}$. The strain introduced by InAsP induces dislocation bending at the InAsP/InP interface, thereby facilitating the reaction and annihilation of dislocations during their lateral glide. Concurrently, the InP spacer exhibits tensile strain, leading to the formation of stacking faults (SFs). With a comprehensive analysis utilizing x-ray diffraction, electron channeling contrast imaging, and transmission electron microscopy, the effects of DFL-induced strain on dislocations and SFs are investigated. Fine-tuning the strain conditions allowed low-dislocation-density while SF-suppressed, anti-phase boundary free InP on Si. This work, therefore, provides a useful buffer engineering scheme for monolithic integration of InP-based electronic and photonic devices onto the industry-standard silicon platform.

OPERA Work Group

WG2 & WG3

Electrical characteristics of Al/AlGaAs/GaAs diode with high-Al concentration at the interface



Reference: J Mater Sci: Mater Electron (2024) 35:189. htps://doi.org/10.1007/s10854-023-11907-4

Authors: HH Gullu, DE Yıldız, M Yıldırım, I Demir, I

Altuntas

Laboratories: Sivas Cumhuriyet University
Nanophotonics Application and Research Center - CUNAM
(Tr), and Microelectronics, Guidance and Electro-Optics
Division, Optical and Optomechanical Design Department,
ASELSAN Inc., (TR)

Techniques: MOVPE, XRD, SEM, Solar Simulator, I-V

Abstract

In this study, GaAs-based Schottky diode is fabricated by Al metal contact and Al0.95Ga0.5As interface layer. Thin film layer is epitaxially grown on GaAs with high ratio of Al in the composition. Compositional, crystallographic structure and surface of the film layer are investigated by in situ reflectance, X-ray diffraction and SEM measurements, respectively. The diode is characterized by room-temperature current—voltage (I-V) measurements under continuous illumination and also transient illumination condition with different intensities in the range of 20–100 mW/cm2. Under bias, the diode shows single Schottky diode characteristics with about two-order rectifying behavior at dark and slight increase in rectification behavior is observed by increasing illumination intensity. Experimental dark and illuminated

curves are formulated by traditional thermionic emission model and the resulting forward biased semi-logarithmic

relations are analyzed to get insight into ideality and barrier height formation. Dark ideality factor and barrier height values are calculated as about 2.32 and 0.64 eV, respectively. Deviation from diode ideality increases with illumination is observed whereas there is a decrease in barrier height of the junction. Saturation from ideal characteristics at high forward bias region is dominated by resistance effect. At this region, series resistance values are evaluated by Cheung's theory. Additionally, switch on/off light response of the diode is observed from transient photo-current measurements for various illumination intensities. Both carrier generation under illumination and trapping mechanism at dark exhibit photo-sensitivity characteristic of the diode. As a result, increase in current flow together with improvement in rectifying behavior with illumination indicates that the diode can be adapted in opto-electronics applications.

OPERA Work Group

WG2&3

Materials: AlGaAs, GaAs